HHS Public Access

Author manuscript

Bioorg Med Chem. Author manuscript; available in PMC 2023 May 15.

Published in final edited form as:

Bioorg Med Chem. 2022 May 15; 62: 116726. doi:10.1016/j.bmc.2022.116726.

Discovery of small-molecule inhibitors of RUVBL1/2 ATPase

Gang Zhang[a,*], **Feng Wang**[a], **Shan Li**[a], **Kai-Wen Cheng**[a], **Yingying Zhu**[b], **Ran Huo**[b], **Elyar Abdukirim**[b], **Guifeng Kang**[b,*], **Tsui-Fen Chou**[a,c,*]

[a]Division of Biology and Biological Engineering, California Institute of Technology, Pasadena, CA 91125, United States

[b]School of Pharmaceutical Sciences, Capital Medical University, Beijing 100069, China

[c]Proteome Exploration Laboratory, Beckman Institute, California Institute of Technology, Pasadena, CA 91125, United States

Abstract

RUVBL1 and RUVBL2 are highly conserved AAA ATPases (ATPases Associated with various cellular Activities) and highly relevant to the progression of cancer, which makes them attractive targets for novel therapeutic anticancer drugs. In this work, docking-based virtual screening was performed to identify compounds with activity against the RUVBL1/2 complex. Seven compounds showed inhibitory activity against the complex in both enzymatic and cellular assays. A series of pyrazolo[1,5-*a*]pyrimidine-3-carboxamide analogs were synthesized based on the scaffold of compound **15** with inhibitory activity and good potential for structural manipulation. Analysis of the structure-activity relationship identified the benzyl group on R_2 and aromatic ring-substituted piperazinyl on R_4 as essential for inhibitory activity against the RUVBL1/2 complex. Of these, compound **18**, which has IC_{50} values of 6.0 ± 0.6 μM and 7.7 ± 0.9 μM against RUVBL1/2 complex and RUVBL1 respectively, showed the most potent inhibition in cell lines A549, H1795, HCT116, and MDA-MB-231 with IC_{50} values of 15 ± 1.2 μM, 15 ± 1.8 μM, 11 ± 1.0 μM, and 8.9 ± 0.9 μM respectively. A docking study of the compound was performed to predict the binding mode of pyrazolo[1,5-*a*]pyrimidine-3-carboxamides. Furthermore, mass spectrometry-based proteomic analysis was employed to explore cellular proteins dysregulated by treatment with compounds **16, 18, and 19**. Together, the data from these analyses suggest that that compound **18** could serve as a starting point for structural modifications in order to improve potency, selectivity, and pharmacokinetic parameters of potential therapeutic molecules.

[*]Corresponding authors. Tel.: +1 626-395-6772. tfchou@caltech.edu (Tsui-Fen Chou); guifengkang@ccmu.edu.cn (Guifeng Kang); gzhang2@caltech.edu (Gang Zhang).

Declaration of competing interest

The authors have no conflicts of interest to declare.

Declaration of interests

The authors declare that they have no known competing financial interests or personal relationships that could have appeared to influence the work reported in this paper.

Appendix A. Supplementary data

Supplementary data to this article can be found online at https://doi.org/xx.xxxx/xxxxxxxxxxxx.

Graphical Abstract

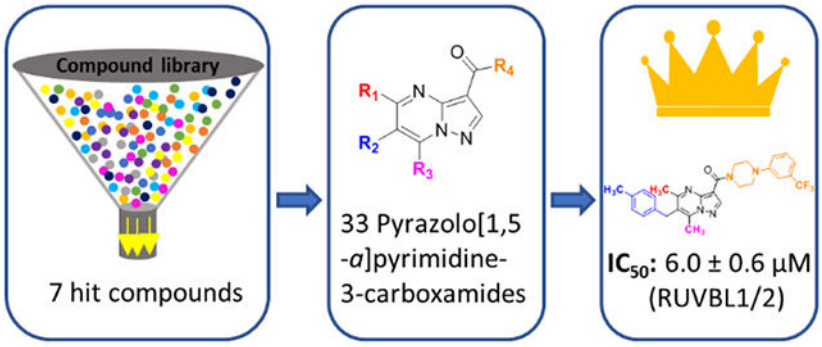

Keywords

RUVBL1; Pontin; RUVBL2; Reptin; AAA ATPase; Organic Synthesis; Docking; pyrazolo[1,5-a] pyrimidine-3-carboxamide; Proteomics

1. Introduction

RUVBL proteins RUVBL1 (TIP49, TIP49a, Rvb1, Pontin) and RUVBL2 (TIP48, TIP49b, Rvb2, Reptin) are present in the Archaea and Eukarya domains, including in humans and fungi. RUVBL proteins are highly conserved AAA proteins (ATPases Associated with various cellular Activities), known to be involved in transcription regulation, DNA damage repair, cell cycle control, and stress adaptation [1-3]. RUVBLs assemble as heteromeric complexes that form an integral component of chromatin remodeling complexes TIP60 [4], INO80 [5] and SWR1/SRCAP [6], as well as of the R2TP chaperone complex [7] and PAQosome [8]. The RuvBL1/2 complex functions as a chaperone itself during the biogenesis of telomerase, H/ACA RNPs and other supramolecular complexes [2, 4, 9, 10]. As well, RuvBL1 and RuvBL2 function independently and even antagonistically in many instances [11-13]. Numerous structural studies indicate that the assembled complex can occur in both hexameric and dodecameric (stacked double hexamer) arrangements [9, 14-17].

There is increasing evidence that the presence of RUVBL1 and RUVBL2 contributes to cancer progression. Overexpression of RUVBL1 and RUVBL2 is observed in many cancer types, including liver, colorectal, breast, gastric, and non-small cell lung cancer [3, 18-22]. Furthermore, multiple studies have suggested that depletion of RUVBLs can hinder cancer cell growth and progression in both in vitro and in vivo models [2, 23, 24]. Combined, this data indicates that RUVBL1 and RUVBL2 may be good targets for anticancer treatment.

Elkaim *et al.* used virtual screen and enzymatic assays to identify four small-molecule inhibitors of RUVBL1 (Akt1/2 inhibitor, PTP1B inhibitor, Rottlerin, and Pranlukast, see Figure 1) [25], which inhibit RUVBL1 with IC_{50} values of 24, 15, 10 and 13 μM, respectively. The mechanism by which their action against RUVBL1 occurs needs to be determined in further study. Encouraged by previously published data from RUVBL1 inhibitors, Elkaim *et al.* focused on two scaffolds, 4-hydroxy-2-pyridone and 4-hydroxy-2-

quinolone, and synthesized derivatives; compounds **5** and **6** (Figure 1) inhibited RUVBL1 activity in an ATP-dependent manner with IC_{50} values of 9 and 18 μM, respectively. Compound **5** demonstrated antiproliferative activity against KB and HL60 cell lines with IC_{50}s of 9 and 15 μM, manifested as apoptotic cell death together with necrosis [26].

Compound **7** (Figure 1) was initially identified as an RUVBL1/2 complex inhibitor with an IC_{50} of 59 nM [27]. In cellular assays, compound **7** depleted PIKK-family members DNA-PKcs (PRKDC), ATM, and ATP, all of which require RUVBL1/2 ATPase activity for stability [28]. Compound **7** was shown to arrest NSCLC cells in S phase, which eventually underwent apoptosis, indicated by the sub-G1 population in DNA content analysis. Sorafenib (Figure 1, Compound **8**) was identified as a RUVBL2 inhibitor with a K_d value of about 22 μM by high-throughput screening [29]. Sorafenib is shown to be an oral multi-kinase inhibitor used to treat advanced renal cell, liver and thyroid cancer [30]. Sorafenib inhibited RUVBL2 in a mixed non-competitive mode and inhibited activity of the RUVBL1/2 complex. Anderson and co-workers identified CB-6644 as a selective, noncompetitive inhibitor of the RUVBL1/2 complex with a IC_{50} value of 15 nM [31]. However, CB-6644 showed a maximal inhibition of only ~50%. Herein, we report the discovery of five pyrazolo[1,5-*a*]pyrimidine-3-carboxamides with the inhibition of RUVBL1/2 ATPase activity and the IC_{50} value of compound **18** is about 6 μM. Mass spectrometry-based proteomic analysis of cells treated with compounds **16, 18, or 19** were completed to compare the cellular pathways affected.

2. Results and Discussion

2.1 Docking-Based virtual Screening

In order to identify novel compounds with anti-RUVBL1/2 activity, docking-based virtual screening was performed using approximately 260,000 compounds from the NCI open compound library. The protein PDB file 5oaf was downloaded from Protein Data Bank (rcsb.org), followed by removal of water molecules and addition of hydrogens in AutoDock 4.2.6 [32]. The coordinates of the Grid center and box size were generated in AutoDock 4.2.6 and the docking results were ranked by binding affinity. Eighty compounds were selected from the top 3000 binding poses after visualization using the BIOVIA Discovery Studio Visualizer 4.5 (Biovia Inc.). In parallel, ligand-based similarity searches in the Swiss Similarity database [33] were performed to screen small molecules from the ChemDiv compound set (around 1,746,000) using CB-6644 as the template molecule. Seventeen compounds (including compounds **16-20**) were selected from the top 500 compounds after evaluating their structures.

2.2 Biological evaluation of compounds from virtual screening

All 97 of the selected compounds were evaluated using an ATPase Assay. Seven of these compounds showed inhibition activity against the RUVBL1/2 complex at an enzymatic level in this work, including compounds **8** and **10-15** (Figure 2, Table 1). Interestingly, after we checked the structures of these compound, we found **8** is known as sorafenib, which was reported as an RUVBL2 inhibitor previously [29]. In addition to activity against the RUVBL1/2 complex, compounds **11, 13, 14**, and **15** showed inhibitory activity against

RUVBL1. Compound **15** was the only compound to show inhibition towards RUVBL1, RUVBL2, and the RUVBL1/2 complex. Next, we used four cancer cell lines to evaluate anti-proliferative effects of these compounds. However, no compound exhibited more potent inhibition than CB-6644 on any of these cell lines (Figure 3). Compounds **8, 12, 13, 14**, and **15** showed moderate inhibitory activity against the RUVBL1/2 complex in enzymatic assays. CB-6644 showed the most potent inhibition in cell lines A549, HCT116, H1795 and MDA-MB-231 (Figure 3). Compared to **14**, compound **15** showed comparable inhibition activity in A549, HCT116, and MDA-MB-231 and more potent inhibition in the H1795 cell line.

2.3 Synthesis of pyrazolo[1,5-a]pyrimidine analogs

Due to the *in vitro* activity and the scaffold that compounds **14** and **15** are sharing, we selected compound **15** as the target compound on which to perform further structural optimization. The pyrazolo[1,5-*a*]pyrimidine-3-carboxamides were synthesized in a three-step sequence of reactions that included cyclization of ethyl pyrazolo[1,5-*a*]pyrimidine-3-carboxylate core, hydrolysis of the ester moiety and amidation (Scheme 1). Specifically, ethyl pyrazolo[1,5-*a*]pyrimidine-3-carboxylate was synthesized by the reaction of ethyl 3-amino-1*H*-pyrazole-4-carboxylate with a series of diketone or dialdehyde compounds (**1a-n**) under acidic conditions. Hydrolysis of these intermediates with sodium hydroxide produced the corresponding carboxylic acids in good yields. For the synthesis of **3a**, boration and benzylation were performed prior to saponification of the ethyl ester of **2a**. Due to the difficulty of its isolation, (3-(ethoxycarbonyl)pyrazolo[1,5-*a*]pyrimidin-6-yl)boronic acid (**2ab**) was used directly for the next step without further purification. To deliver the final target compounds (**21-48**), the substituted pyrazolo[1,5-*a*]pyrimidine-3-carboxylic acids were coupled with substituted amines. Compound **47** was obtained by deprotection of Boc in the presence of hydrogen chloride; it was further derivatized into compound **48** through propargylation reactions with propargyl bromide.

2.4 Structure-Activity Relationship of pyrazolo[1,5-a]pyrimidine-3-carboxamide analogs

All of the pyrazolo[1,5-*a*]pyrimidine-3-carboxamides, including **16-20** from the ChemDiv compound library and the synthesized target compounds **21-48**, were evaluated for the inhibitory activity against the RUVBL1/2 complex (Table S1). Among these compounds, Compound **18** showed the most potent inhibition against RUVBL1/2 with an IC_{50} value of 6.0 ± 0.6 μM. Additionally, **18** could inhibit RUVBL1 with an IC_{50} value of 7.7 ± 0.9 μM. Methyl groups on R_1 and R_3 were favorable for inhibitory activity; their replacement by H led to the loss of inhibition (Compound **23**). As the volume of the hydrophobic group increases ($CH_3 \rightarrow CH_2CH_3$), the inhibitory potency decreases (Compounds **18** → **22** → **21**). The substituted benzyl on R_2 is essential to the inhibitory activity as the H atom and alkyl groups on R_2 resulted in the loss of the inhibitory activity (compounds **20, 31**, and **32**). The methyl group on the ortho-position of benzyl group led to the loss of the activity against RUVBL1/2 (compound **28**). The aromatic-substituted piperazinyl on R_4 is essential to the inhibitory activity. However, the heteroaromatic ring-substituted on piperazine decrease the activity compared to the phenyl ring (**17** vs **16**). When R_4 is the amino group substituted by H (compound **42**), alky (compounds **43** and **45**) or aryl (compound **44**) groups, the activity

of these compounds decreases greatly. The CF_3-substituted on the ortho-position of phenyl ring (on piperazinyl) led to the loss of the activity (compound **34**).

2.5 Proposed binding mode of compound 18

To investigate the binding mode of pyrazolo[1,5-*a*]pyrimidine-3-carboxamide analogs, we performed a docking study of compound **18** with the RUVBL1/2 complex. Residue Arg378 showed interactions with compound **18** by hydrogen bonds. His18 interacted with the pyrimidine ring of compound **18** by a cation-π interaction. Arg404 showed cation-π interactions with the pyrazolo and pyrimidine of compound **18**. There was a potential halogen bond (with 2.9 Å) between the CF_3 group and Val40. Multiple residues, such as Leu39, Ala78, Leu79, and the carbon atoms on the side chains of Glu317 and Arg353, showed hydrophobic interactions with these two terminal phenyl rings of compound **18**, which is consistent with the study of the structure-activity relationship described above.

2.6 Cytotoxicity of pyrazolo[1,5-a]pyrimidine-3-carboxamide analogs

To determine the cellular activity of pyrazolo[1,5-*a*]pyrimidine-3-carboxamides, we performed the CellTiter-Glo Luminescent Cell Viability Assay. CB-6644 showed more potent cytotoxicity in the nanomolar IC_{50} range than did compounds **16-19**. Among the pyrazolo[1,5-*a*]pyrimidine-3-carboxamides, compound **18** was identified as the compound with the most potent cytotoxicity against cell lines A549, HCT116, H1795, and MDA-MB-231 (Table 2 and Figure S1).

2.7 Quantitative Proteomics Analysis of compounds 16, 18, and 19 in treatment of HCT116 human colon cancer cells

To further study the cellular effects of compounds **16, 18**, and **19** and determine which proteins are selectively altered upon treatment, we performed mass spectrometry-based proteomics analysis in HCT116 cells. We evaluated proteome changes using DMSO as negative control after 24 h treatment with either compound **16, 18** or **19**. We identified a total of 7693 proteins, among which 268, 229 and 164 were dysregulated by compounds **16, 18** and **19**, respectively ($P < 0.05$, $|Log_2FC|>0.5$) (Figure 5A-C). Of these dysregulated proteins, 193, 112, and 117 were downregulated (Figure 5E). We performed heatmap analysis for differentially expressed proteins identified from two out of three compounds treated groups ($p < 0.05$, $|Log_2FC|>0.5$) (Figure 5F). The dysregulated proteins from compounds **16, 18**, and **19** showed the same trend in the heatmap analysis (Figure 5F). Comparative analysis showed 13 and 30 proteins respectively that were exclusively upregulated and downregulated by pyrazolo[1,5-*a*]pyrimidine-3-carboxamides **16, 18**, and **19** (Figure 5D, Tables S2 and S3).

2.8 GO and KEGG pathway analysis of differentially expressed proteins

To better understand the biological functions of the differentially expressed proteins, we performed GO enrichment and KEGG pathway analyses (Figure 6). The four most significant processes identified by GO analysis annotations of biological process (BP) were regulation of mitotic cell cycle, cell division, cell proliferation, and response to cytokine. The two most significant processes identified among the annotations of cellular

component (CC) was nucleus and extracellular space. Two most significant processes identified among annotations of molecular function (MF) were kinase activity and DNA binding. Signaling pathway enrichment analysis of the differentially expressed proteins identified two meaningful pathways with P-value<0.05, namely proteoglycans in cancer and the HIF-1 signaling pathway. Our pathway analysis results were consistent with the various roles of RUVBL1/2 ATPase in regulating cell proliferation, cell cycle [34], regulate chromatin complexes [35] and DNA replication [36]. In our recent review [37], several published studies are referenced to discuss that RUVBL1 and 2 are involved in many cellular activities that are also enriched in our inhibitors induced pathway analysis.

3. Conclusion

RUVBL1 and RUVBL2 are well-known drug targets that assemble into heterohexameric rings. Beginning with docking-based virtual screening, 97 compounds were selected and their inhibition activity against RUVBL1/2 complex was evaluated. Seven compounds showed inhibitory activity against the RUVBL1/2 complex in both enzymatic and cellular assays. Due to the chemical space and observed activity, compound **15** was selected as the hit compound for further structural optimization due to its ability to inhibit RUVBL1 and RUVBL2 in addition to the RUVBL1/2 complex. In order to study the structure-activity relationship, a series of pyrazolo[1,5-*a*]pyrimidine-3-carboxamides (28 synthesized compounds and 10 selected compounds purchased from ChemDiv) were evaluated. Structure-activity relationship analysis suggested that the substituted benzyl on R_2 and the aromatic-substituted piperazinyl on $R_4$are essential to the RUVBL1/2 inhibition. Compounds **16, 18**, and **19** showed potent inhibition of both enzymatic and cellular activity. The proposed binding mode of compound **18** by docking implied the involvement of hydrophobic interactions between the active residues and the substituents on R_2 andR_4. MS-based proteomics identified 13 and 30 proteins were up- and down-regulated respectively by pyrazolo[1,5-*a*]pyrimidine-3-carboxamides **16, 18**, and **19**. Compound **18** could be used as a lead compound for further therapeutic development.

4. Materials and Methods

4.1 Chemical Synthesis

4.1.1 Materials—All solvents and chemical reagents were purchased from commercial sources and used directly without further purification. The progress of all reactions was monitored by analytical thin-layer chromatography on silica gel 60 F_{254} plates (Merck). The purification by column chromatography was performed using 200-300 mesh silica gel (Qingdao Haiyang Chemical Co. Ltd.). ^{1}H-NMR spectra were recorded on a Bruker AVANCE 300 or 500 MHz spectrometer in DMSO-d_6. ^{13}C-NMR spectra were recorded on a Bruker AVANCE 75 or 125 MHz spectrometer in DMSO-d_6. Chemical shift values were reported in δ values parts per million (ppm), referenced to dimethyl sulfoxide (DMSO) using the residual solvent signal as an internal reference. High-resolution mass spectrometry data (HRMS) were recorded on the ICR (Fourier transform ion cyclotron resonance, FTICR) analyzer using an ESI source. Infrared spectra (IR) were recorded on a Thermo Scientific Nicolet iS5 FT-IR spectrophotometer and reported as wavelength numbers (cm^{-1}). Melting

points were determined with an X-4A microscopic melting point apparatus, which was uncorrected. All of the test compounds exhibited >95% purity as determined by HPLC. HPLC analysis was performed using an Agilent HPLC 1200 system (column, Agilent C18, 4.6 mm × 150 mm, 5 μm).

4.1.2 General Procedure for the Synthesis of ethyl pyrazolo[1,5-*a*]pyrimidine-3-carboxylates (2a-n).—

The mixture of ethyl 3-amino-1*H*-pyrazole-4-carboxylate (775 mg, 5.0 mmol, 1.0 eq.) and diketone or dialdehyde compounds (5.25 mmol, 1.05 eq.) in AcOH (4 mL) and EtOH (4 mL) was stirred at 70 °C for 3 h. The mixture was concentrated *in vacuo* and then partitioned between 50 mL EtOAc and 50 mL $NaHCO_3$ aqueous solution. The organic layer was collected, and the aqueous phase was extracted with 30 mL EtOAc. The combined organic phases were dried over anhydrous Na_2SO_4 and concentrated *in vacuo*. The residues were purified by column chromatography (silica gel, petroleum ether (b.p. 60-90 °C)/ethyl acetate, 20:1 to 3:1) to obtain the intermediates.

Ethyl 6-bromopyrazolo[1,5-a]pyrimidine-3-carboxylate (2aa).: Yield: 60%. Yellow solid. M.P. 140.7-142.8 °C. ^{1}H NMR (300 MHz, DMSO-d_6) δ (ppm): 9.75 (d, J = 2.1 Hz, 1 H), 8.89 (d, J = 2.1 Hz, 1 H), 8.59 (s, 1 H), 4.28 (q, J = 7.0 Hz, 2 H), 1.29 (t, J = 7.0 Hz, 3 H). ^{13}C NMR (75 MHz, DMSO-d_6) δ (ppm): 161.4, 153.7, 147.7, 145.2, 137.4, 105.7, 102.3, 59.8, 14.4. IR ν_{max} (neat): 3062, 2976, 1708, 1539, 1375, 1259, 1209, 1195, 1050, 902, 806, 782, 695. HRMS (ESI+): *m/z* $[2M+Na]^+$ calcd. for $C_{18}H_{16}Br_2N_6O_4Na^+$, 560.9492; found, 560.9492 (error 0 ppm).

Ethyl 6-benzylpyrazolo[1,5-a]pyrimidine-3-carboxylate (2a).: A mixture of ethyl 6-bromopyrazolo[1,5-*a*]pyrimidine-3-carboxylate **2aa** (2.0 g, 7.4 mmol, 1.0 eq.), Bis(pinacolato)diboron (2.26 g, 8.8 mmol, 1.2 eq.), KOAc (2.18 g, 22.2 mmol, 3.0 eq.) and 1,1'-bis(diphenylphosphino)ferrocene-palladium(II)dichloride complex with DCM (0.42 g, 0.52 mmol, 0.07 eq.) in dioxane (40 mL) was stirred at 80 °C overnight. The reaction mixture was allowed to cool to room temperature and partitioned between 50 mL EtOAc and 50 mL 2M HCl. The aqueous layer was extracted twice with 30 mL EtOAc and the combined organic layers were concentrated *in vacuo*. The residue was dissolved in 50 mL EtOAc and 50 mL 2M NaOH was added. After separation, the aqueous layer was acidified with hydrochloric acid and extracted with EtOAc (50 mL×3). The combined organic layer was dried over Na_2SO_4 and concentrated *in vacuo* to give the crude product **2ab** (1.13 g, 4.8 mmol, 65%) as white solid, which was subjected to the next reaction without further purification.

A mixture of (3-(ethoxycarbonyl)pyrazolo[1,5-*a*]pyrimidin-6-yl)boronic acid **2ab** (1.13 g, 4.8 mmol,1.0 eq.), benzyl bromide (0.84 g, 4.8 mmol, 1.0 eq.), and 1,1'-bis(diphenylphosphino)ferrocene-palladium(II)dichloride complex with DCM (0.39 g, 0.48 mmol, 0.1 eq.) in dioxane (30 mL) was treated with a solution of K_2CO_3 (1.32 g, 9.6 mmol, 2.0 eq.) in H_2O (6 mL). The reaction mixture was stirred at 50 °C overnight. The reaction mixture was allowed to cool to room temperature and partitioned between 50 mL EtOAc and 50 mL H_2O. The aqueous layer was extracted twice with 30 mL EtOAc. The combined organic layers were dried over anhydrous Na_2SO_4 followed by filtration and solvent removal *in vacuo*. The residue was purified by column chromatography (silica gel, petroleum ether

(b.p. 60-90 °C)/ethyl acetate, 20:1 to 2:1) to give **2a**. (643 mg, 2.28 mmol) Yield: 47%. White solid. M.P. 121.3-123.0 °C. ^{1}H NMR (300 MHz, DMSO-d_6) δ (ppm): 9.23 (s, 1H), 8.78 (m, 1H), 8.57 (s, 1H), 7.28-7.35 (m, 4H), 7.19-7.24 (m, 1H), 4.27 (q, J = 7.0 Hz, 2H), 4.08 (s, 2H), 1.28 (t, J = 7.0 Hz, 3H). ^{13}C NMR (75 MHz, DMSO-d_6) δ (ppm): 161.6, 155.0, 147.1, 145.7, 139.4, 135.1, 128.7, 128.6, 126.5, 123.9, 101.6, 59.5, 34.5, 14.4. IR ν_{max} (neat): 3051, 2989, 2952, 2930, 1802, 1704, 1629, 1553, 1513, 1389, 1198, 1058, 786, 699. HRMS (ESI+): *m/z* [2M+Na]$^{+}$ calcd. for $C_{32}H_{30}N_6O_4Na^{+}$, 585.2221; found, 585.2210 (error 1.84 ppm).

Ethyl 6-ethyl-5,7-dimethylpyrazolo[1,5-a]pyrimidine-3-carboxylate (2b).: Yield: 51%. White solid. M.P. 107.9-109.4 °C. ^{1}H NMR (300 MHz, DMSO-d_6) δ (ppm): 8.46 (s, 1H), 4.26 (q, J = 7.0 Hz, 2H), 2.67-2.73 (m, 5H), 2.60 (s, 3H), 1.30 (t, J = 7.0 Hz, 3H), 1.11 (t, J = 7.4 Hz, 3H). ^{13}C NMR (75 MHz, DMSO-d_6) δ (ppm): 161.8, 161.7, 145.9, 145.2, 143.8, 122.5, 100.6, 59.3, 23.3, 20.7, 14.4, 13.5, 13.0. IR ν_{max} (neat): 2971, 2940, 2879, 1705, 1616, 1546, 1527, 1371, 1191, 1106, 1025, 786, 639. HRMS (ESI+): *m/z* [2M+Na]$^{+}$ calcd. for $C_{26}H_{34}N_6O_4Na^{+}$, 517.2534; found, 517.2534 (error 0 ppm).

Ethyl 5,7-dimethyl-6-phenylpyrazolo[1,5-a]pyrimidine-3-carboxylate (2c).: Yield: 72%. White solid. M.P. 109.9-110.9 °C. ^{1}H NMR (300 MHz, DMSO-d_6) δ (ppm): 8.58 (s, 1H), 7.49-7.55 (m, 3H), 7.39-7.41 (m, 2H), 4.29 (q, J = 7.0 Hz, 2H), 2.47 (s, 3H), 2.31 (s, 3H), 1.32 (t, J = 7.0 Hz, 3H). ^{13}C NMR (75 MHz, DMSO-d_6) δ (ppm): 161.8, 161.0, 146.6, 145.8, 144.3, 134.7, 129.9, 128.9, 128.4, 123.5, 101.0, 59.4, 24.7, 15.0, 14.4. IR ν_{max} (neat): 3112, 3051, 2977, 1693, 1612, 1386, 1373, 1289, 1207, 1108, 779, 705, 649. HRMS (ESI+): *m/z* [2M+Na]$^{+}$ calcd. for $C_{34}H_{34}N_6O_4Na^{+}$, 613.2534; found, 613.2523 (error 1.75 ppm).

Ethyl 6-benzyl-5,7-dimethylpyrazolo[1,5-a]pyrimidine-3-carboxylate (2d).: Yield: 92%. White solid. M.P. 170.8-172.3 °C. ^{1}H NMR (300 MHz, DMSO-d_6) δ (ppm): 8.54 (s, 1H), 7.26-7.31 (m, 2H), 7.18-7.22 (m, 1H), 7.11-7.13 (m, 2H), 4.27 (q, J = 7.0 Hz, 2H), 4.19 (s, 2H), 2.78 (s, 3H), 2.48 (s, 3H), 1.30 (t, J = 7.0 Hz, 3H). ^{13}C NMR (75 MHz, DMSO-d_6) δ (ppm): 162.4, 161.8, 146.1, 145.5, 145.2, 138.3, 128.7, 127.9, 126.4, 119.4, 100.9, 59.3, 32.6, 23.8, 14.5, 13.8. IR ν_{max} (neat): 3108, 3083, 3002, 2981, 1679, 1617, 1544, 1196, 1121, 781, 724. HRMS (ESI+): *m/z* [2M+Na]$^{+}$ calcd. for $C_{36}H_{38}N_6O_4Na^{+}$, 641.2847; found, 641.2847 (error 0 ppm).

Ethyl 5,7-dimethyl-6-(4-methylbenzyl)pyrazolo[1,5-a]pyrimidine-3-carboxylate (2e).: Yield: 66%. White solid. M.P. 103.7-105.9 °C. ^{1}H NMR (300 MHz, DMSO-d6) δ (ppm): 8.51 (s, 1H), 7.06 (d, J = 7.9 Hz, 2H), 6.97 (d, J = 7.9 Hz, 2H), 4.27 (q, J = 7.0 Hz, 2H), 4.10 (s, 2H), 2.75 (s, 3H), 2.46 (s, 3H), 2.22 (s, 3H), 1.30 (t, J = 7.0 Hz, 3H). ^{13}C NMR (75 MHz, DMSO-d6) δ (ppm): 162.3, 161.8, 146.0, 145.5, 145.0, 135.0, 129.2, 127.6, 119.5, 100.9, 59.2, 32.2, 23.7, 20.5, 14.4, 13.6. IR ν_{max} (neat): 2973, 1720, 1686, 1617, 1550, 1513, 1422, 1370, 1223, 1180, 1107, 974, 838, 780. HRMS (ESI+): m/z [2M+Na]$^{+}$ calcd. for $C_{38}H_{42}N_6O_4Na^{+}$, 669.3160; found, 669.3160 (error 0 ppm).

Ethyl 5,7-dimethyl-6-(3-methylbenzyl)pyrazolo[1,5-a]pyrimidine-3-carboxylate (2f).: Yield: 82%. White solid. M.P. 115.3-116.7 °C. ^{1}H NMR (300 MHz, DMSO-d_6) δ (ppm): 8.51 (s, 1H), 7.12-7.17 (m, 1H), 6.98-7.01 (m, 1H), 6.87-6.92 (m, 2H), 4.27 (q, J =

7.0 Hz, 2H), 4.12 (s, 2H), 2.76 (s, 3H), 2.47 (s, 3H), 2.22 (s, 3H), 1.30 (t, J = 7.0 Hz, 3H). ^{13}C NMR (75 MHz, DMSO-d_6) δ (ppm): 162.3, 161.8, 146.0, 145.5, 145.1, 138.1, 137.8, 128.5, 128.3, 127.0, 124.9, 119.4, 100.9, 59.3, 32.6, 23.8, 20.9, 14.4, 13.7. IR ν_{max} (neat): 2967, 1712, 1615, 1548, 1372, 1355, 1295, 1246, 1190, 1109, 1027, 975, 836, 792, 690. HRMS (ESI+): *m/z* [*M*+H]$^+$ calcd. for $C_{19}H_{22}N_3O_2^+$, 324.1707; found, 324.1715 (error −2.61 ppm).

Ethyl 5,7-dimethyl-6-(2-methylbenzyl)pyrazolo[1,5-a]pyrimidine-3-carboxylate (2g).: Yield: 83%. White solid. M.P. 153.4-154.5 °C. ^{1}H NMR (300 MHz, DMSO-d_6) δ (ppm): 8.54 (s, 1H), 7.22-7.25 (m, 1H), 7.09-7.14 (m, 1H), 6.97-7.02 (m, 1H), 6.50-6.53 (m, 1H), 4.28 (q, J = 7.0 Hz, 2H), 4.05 (s, 2H), 2.68 (s, 3H), 2.43 (s, 3H), 2.411 (s, 3H), 1.31 (t, J = 7.0 Hz, 3H). ^{13}C NMR (75 MHz, DMSO-d_6) δ (ppm): 162.4, 161.8, 146.0, 145.6, 145.4, 136.1, 130.0, 126.2, 126.1, 125.8, 118.8, 100.9, 59.3, 30.1, 23.4, 19.3, 14.4, 13.5. IR ν_{max} (neat): 2984, 1678, 1618, 1544, 1477, 1381, 1229, 1198, 1122, 1022, 785, 750. HRMS (ESI+): *m/z* [*M*+H]$^+$ calcd. for $C_{19}H_{22}N_3O_2^+$, 324.1707; found, 324.1715 (error −2.61 ppm).

Ethyl 6-(4-isopropylbenzyl)-5,7-dimethylpyrazolo[1,5-a]pyrimidine-3-carboxylate (2h).: Yield: 87%. White solid. M.P. 121.5-123.4 °C. ^{1}H NMR (300 MHz, DMSO-d_6) δ (ppm): 8.52 (s, 1H), 7.13 (d, J = 8.0 Hz, 2H), 7.01 (d, J = 8.0 Hz, 2H), 4.27 (q, J = 7.0 Hz, 2H), 4.12 (s, 2H), 2.78-2.87 (m, J = 6.8Hz, 1H), 2.76 (s, 3H), 2.48 (s, 3H), 1.30 (t, J = 7.0 Hz, 3H), 1.14 (d, J = 6.9 Hz, 6H). ^{13}C NMR (75 MHz, DMSO-d_6) δ (ppm): 162.3, 161.8, 146.4, 146.1, 145.5, 145.1, 135.5, 127.7, 126.5, 119.5, 100.9, 59.3, 32.9, 32.2, 23.8, 14.4, 13.7. IR ν_{max} (neat): 3107, 2959, 1678, 1614, 1541, 1515, 1379, 1224, 1198, 1124, 1026, 847, 782. HRMS (ESI+): *m/z* [*M*+H]$^+$calcd. for $C_{21}H_{26}N_3O_2^+$, 352.2020; found, 352.2028 (error −2.40 ppm).

Ethyl 6-(4-methoxybenzyl)-5,7-dimethylpyrazolo[1,5-a]pyrimidine-3-carboxylate (2i).: Yield: 83%. White solid. M.P. 115.0-116.6 °C. ^{1}H NMR (300 MHz, DMSO-d_6) δ (ppm): 8.53 (s, 1H), 7.03 (d, J = 8.6 Hz, 2H), 6.83 (d, J = 8.6 Hz, 2H), 4.27 (q, J = 7.0 Hz, 2H), 4.10 (s, 2H), 3.70 (s, 3H), 2.77 (s, 3H), 2.48 (s, 3H), 1.30 (t, J = 7.0 Hz, 3H). ^{13}C NMR (75 MHz, DMSO-d_6) δ (ppm): 162.4, 161.8, 157.8, 146.1, 145.5, 145.0, 129.9, 128.9, 119.8, 114.1, 100.8, 59.3, 55.0, 31.8, 23.8, 14.4, 13.7. IR ν_{max} (neat): 2977, 2936, 1720, 1615, 1549, 1514, 1383, 1370, 1116, 1027, 842, 785. HRMS (ESI+): *m/z* [2*M*+Na]$^+$ calcd. for $C_{38}H_{42}N_6O_6Na^+$, 701.3058; found, 701.3058 (error 0 ppm).

Ethyl 6-(4-fluorobenzyl)-5,7-dimethylpyrazolo[1,5-a]pyrimidine-3-carboxylate (2j).: Yield: 73%. White solid. M.P. 119.9-122.3 °C. ^{1}H NMR (300 MHz, DMSO-d_6) δ (ppm): 8.52 (s, 1H), 7.14-7.19 (m ,2H), 7.06-7.12 (m, 2H), 4.27 (q, J = 7.0 Hz, 2H), 4.17 (s, 2H), 2.77 (s, 3H), 2.47 (s, 3H), 1.30 (t, J = 7.0 Hz, 3H). ^{13}C NMR (75 MHz, DMSO-d_6) δ (ppm): 162.2, 161.7, 160.7 (d, J = 240.7 Hz), 146.0, 145.4, 145.2, 134.2 (d, J = 2.8 Hz), 129.6 (d, J = 7.9 Hz), 119.2, 115.2 (d, J = 21.0 Hz), 59.2, 31.8, 23.7, 14.4, 13.7. ^{19}F NMR (282 MHz, DMSO-d_6) δ (ppm): −116.7. HRMS (ESI+): *m/z* [*M*+H]$^+$ calcd. for $C_{18}H_{19}FN_3O_2^+$, 328.1456; found, 328.1463 (error −2.19 ppm).

Ethyl 6-(4-chlorobenzyl)-5,7-dimethylpyrazolo[1,5-a]pyrimidine-3-carboxylate (2k).: Yield: 83%. White solid. M.P. 137.8-140.0 °C. ^{1}H NMR (300 MHz, DMSO-d_6) δ (ppm): 8.52 (s, 1H), 7.32 (d, J = 8.3 Hz, 2H), 7.15 (d, J = 8.3 Hz, 2H), 4.27 (q, J = 7.0 Hz, 2H), 4.17 (s, 2H), 2.76 (s, 3H), 2.46 (s, 3H), 1.30 (t, J = 7.0 Hz, 3H). ^{13}C NMR (75 MHz, DMSO-d_6) δ (ppm): 162.2, 161.8, 146.1, 145.6, 145.4, 137.3, 131.0, 129.7, 128.5, 119.0, 100.9, 59.3, 32.0, 23.8, 14.4, 13.7. IR ν_{max} (neat): 2983, 2897, 1709, 1614, 1550, 1372, 1292, 1242, 1187, 1109, 984, 796, 783. HRMS (ESI+): *m/z* [2*M*+Na]$^{+}$ calcd. for $C_{36}H_{36}Cl_2N_6O_4Na^{+}$, 709.2067; found, 709.2067 (error 0 ppm).

Ethyl 5,7-dimethyl-6-(4-(trifluoromethyl)benzyl)pyrazolo[1,5-a]pyrimidine-3-carboxylate (2l).: Yield: 84%. White solid. M.P. 143.8-144.4 °C. ^{1}H NMR (300 MHz, DMSO-d_6) δ (ppm): 8.54 (s, 1H), 7.63 (d, J = 8.0 Hz, 2H), 7.37 (d, J = 8.0 Hz, 2H), 4.24-4.30 (m, 4H), 2.78 (s, 3H), 2.47 (s, 3H), 1.30 (t, J = 7.0 Hz, 3H). ^{13}C NMR (75 MHz, DMSO-d_6) δ (ppm): 162.2, 161.7, 146.1, 145.6, 145.5, 143.3, 128.7, 127.1 (q, J = 31.5 Hz), 125.3 (q, J = 3.5 Hz), 124.2 (q, J = 270.2 Hz), 118.5, 100.9, 59.2, 32.5, 23.8, 14.4, 13.7. ^{19}F NMR (282 MHz, DMSO-d_6) δ (ppm): −60.9. IR ν_{max} (neat): 2984, 1714, 1616, 1551, 1522, 1374, 1320, 1244, 1163, 1108, 813, 783. HRMS (ESI+): *m/z* [*M*+H]$^{+}$ calcd. for $C_{19}H_{19}F_3N_3O_2^{+}$, 378.1424; found, 378.1433 (error −2.41 ppm).

Ethyl 5-ethyl-7-methyl-6-(4-methylbenzyl)pyrazolo[1,5-a]pyrimidine-3-carboxylate (2m).: Yield: 58%. White solid. M.P. 121.3-124.1 °C. ^{1}H NMR (300 MHz, DMSO-d_6) δ (ppm): 8.54 (s, 1H), 7.09 (d, J = 7.8 Hz, 2H), 6.98 (d, J = 7.8 Hz, 2H), 4.27 (q, J = 7.0 Hz, 2H), 4.14 (s, 2H), 3.20 (q, J = 7.3 Hz, 2H), 2.46 (s, 3H), 2.24 (s, 3H), 1.30 (t, J = 7.0 Hz, 3H), 1.14 (t, J = 7.3 Hz, 3H). ^{13}C NMR (75 MHz, DMSO-d_6) δ (ppm):162.9, 161.7, 149.3, 146.1, 145.6, 135.3, 129.2, 127.6, 118.6, 100.8, 59.2, 31.8, 23.8, 20.6, 20.4, 14.4, 10.9. IR ν_{max} (neat): 2969, 2936, 2873, 1716, 1609, 1548, 1514, 1370, 1347, 1291, 1190, 1121, 1090, 788. HRMS (ESI+): *m/z* [*M*+H]$^{+}$ calcd. for $C_{20}H_{24}N_3O_2^{+}$, 338.1863; found, 338.1870 (error −2.06 ppm).

Ethyl 5,7-diethyl-6-(4-methylbenzyl)pyrazolo[1,5-a]pyrimidine-3-carboxylate (2n).: Yield: 55%. White solid. M.P. 82.9-84.8 °C. ^{1}H NMR (300 MHz, DMSO-d_6) δ (ppm): 8.54 (s, 1H), 7.07 (d, J = 7.8 Hz, 2H), 6.96 (d, J = 7.8 Hz, 2H), 4.26 (q, J = 7.0 Hz, 2H), 4.15 (s, 2H), 3.19 (q, J = 7.2 Hz, 2H), 2.76 (q, J = 7.2 Hz, 2H), 2.23 (s, 3H), 1.30 (t, J = 7.0 Hz, 3H), 1.11-1.20 (m, 6H). ^{13}C NMR (75 MHz, DMSO-d_6) δ (ppm): 166.1, 161.8, 149.2, 146.1, 145.8, 135.6, 135.3, 129.1, 127.5, 118.1, 101.0, 59.2, 31.2, 28.3, 20.7, 20.5, 14.3, 11.3, 10.9. IR ν_{max} (neat): 2969, 1716, 1611, 1544, 1513, 1467, 1369, 1349, 1237, 1120, 1091, 928, 911, 795, 780. HRMS (ESI+): *m/z* [*M*+H]$^{+}$ calcd. for $C_{21}H_{26}N_3O_2^{+}$, 352.2020; found, 352.2019 (error 0.15 ppm).

4.1.3 General Procedure for the Synthesis of pyrazolo[1,5-a]pyrimidine-3-carboxylic acids (3a-n)—

To a solution of ethyl pyrazolo[1,5-*a*]pyrimidine-3-carboxylates (4.0 mmol, 1.0 eq.) in THF (3.0 mL) and MeOH (3.0 mL) was added 2 M NaOH aqueous solution (3.0 mL, 6.0 mmol, 1.5 eq.). The mixture was stirred at 56 °C for 3 h and then concentrated *in vacuo*. The residue was suspended in water, and 2 M HCl aqueous solution (3.0 mL, 6.0 mmol, 1.5 eq.) was added. The resulting solid was

collected by filtration, rinsed with water, and dried to afford the intermediates as off-white to yellowish solids.

6-benzylpyrazolo[1,5-a]pyrimidine-3-carboxylic acid (3a).: Yield: 81%. Pale yellow solid. M.P. 237.3-240.1 °C. ^{1}H NMR (300 MHz, DMSO-d_6) δ (ppm): 12.39 (s, 1H), 9.20 (s, 1H), 8.74 (s, 1H), 8.54 (s, 1H), 7.28-7.33 (m, 4H), 7.21-7.23 (m, 1H), 4.08 (s, 2H). ^{13}C NMR (75 MHz, DMSO-d_6) δ (ppm): 163.1, 154.7, 147.4, 145.8, 139.5, 135.0, 128.7, 128.6, 126.6, 123.7, 102.4, 34.5. IR ν_{max} (neat): 3079, 2921, 1698, 1626, 1558, 1521, 1413, 1386, 1269, 1196, 1049, 778, 721, 641. HRMS (ESI−): *m/z* [2M-H]$^-$ calcd. for $C_{28}H_{21}N_6O_4^-$, 505.1630; found, 505.1620 (error 1.94 ppm).

6-ethyl-5,7-dimethylpyrazolo[1,5-a]pyrimidine-3-carboxylic acid (3b).: Yield: 88%. Pale yellow solid. M.P. 179.5-180.9 °C. ^{1}H NMR (500 MHz, DMSO-d_6) δ (ppm): 12.11 (s, 1H), 8.43 (s, 1H), 2.70-2.74 (m, 5H), 2.61 (s, 3H), 1.13 (t, J = 7.5 Hz, 3H). ^{13}C NMR (125 MHz, DMSO-d_6) δ (ppm): 163.2, 161.2, 146.2, 145.1, 143.7, 122.2, 101.3, 23.1, 20.6, 13.4, 12.9. IR ν_{max} (neat): 2972, 2579, 1717, 1643, 1613, 1538, 1523, 1361, 1232, 1190, 784, 733, 657, 640. HRMS (ESI+): *m/z* [2M+Na]$^+$ calcd. for $C_{22}H_{26}N_6O_4Na^+$, 461.1908; found, 461.1908 (error 0 ppm).

5,7-dimethyl-6-phenylpyrazolo[1,5-a]pyrimidine-3-carboxylic acid (3c).: Yield: 82%. White solid. M.P. 220.0-221.9 °C. ^{1}H NMR (300 MHz, DMSO-d_6) δ (ppm): 12.31 (brs, 1H), 8.54 (s, 1H), 7.45-7.56 (m, 3H), 7.38-7.41 (m, 2H), 2.47 (s, 3H), 2.30 (s, 3H). ^{13}C NMR (75 MHz, DMSO-d_6) δ (ppm): 163.4, 160.6, 147.0, 145.8, 144.3, 134.9, 129.9, 128.9, 128.4, 123.2, 101.9, 24.6, 15.0. IR ν_{max} (neat): 3061, 2697, 2631, 2577, 1714, 1658, 1610, 1513, 1386, 1233, 1198, 788, 702. HRMS (ESI+): *m/z* [2M+Na]$^+$ calcd. for $C_{30}H_{26}N_6O_4Na^+$, 557.1908; found, 557.1908 (error 0 ppm).

6-benzyl-5,7-dimethylpyrazolo[1,5-a]pyrimidine-3-carboxylic acid (3d).: Yield: 85%. White solid. M.P. 180.5-182.9 °C. ^{1}H NMR (500 MHz, DMSO-d_6) δ (ppm): 12.16 (s, 1H), 8.49 (s, 1H), 7.26-7.29 (m, 2H), 7.19 (t, J = 7.3 Hz, 1H), 7.11-7.12 (m, 2H), 4.18 (s, 2H), 2.77 (s, 3H), 2.47 (s, 3H). ^{13}C NMR (125 MHz, DMSO-d_6) δ (ppm): 163.3, 162.0, 146.4, 145.5, 145.1, 138.3, 128.6, 127.8, 126.3, 119.2, 101.6, 32.6, 23.7, 13.7. IR ν_{max} (neat): 2945, 1727, 1660, 1615, 1553, 1493, 1362, 1248, 1198, 784, 736, 701. HRMS (ESI−): *m/z* [*M*-H]$^-$ calcd. for $C_{16}H_{14}N_3O_2^-$, 280.1092; found, 280.1092 (error 0 ppm).

5,7-dimethyl-6-(4-methylbenzyl)pyrazolo[1,5-a]pyrimidine-3-carboxylic acid (3e).: Yield: 90%. White solid. M.P. 192.0-193.8 °C. ^{1}H NMR (300 MHz, DMSO-d_6) δ (ppm): 12.58 (brs, 1H), 8.48 (s, 1H), 7.07 (d, J = 7.7 Hz, 2H), 6.98 (d, J = 7.7 Hz, 2H), 4.11 (s, 2H), 2.76 (s, 3H), 2.46 (s, 3H), 2.23 (s, 3H). ^{13}C NMR (75 MHz, DMSO-d_6) δ (ppm): 163.8, 161.8, 146.4, 145.3, 144.9, 135.3, 135.1, 129.2, 127.6, 119.1, 102.4, 32.2, 23.6, 20.5, 13.7. IR ν_{max} (neat): 2921, 1660, 1616, 1548, 1515, 1493, 1386, 1360, 1248, 1195, 944, 785. HRMS (ESI−): *m/z* [*M*-H]$^-$ calcd. for $C_{17}H_{16}N_3O_2^-$, 294.1248; found, 294.1253 (error −1.70 ppm).

5,7-dimethyl-6-(3-methylbenzyl)pyrazolo[1,5-a]pyrimidine-3-carboxylic acid (3f).: Yield: 84%. White solid. M.P. 180.5-183.1 °C. ^{1}H NMR (300 MHz, DMSO-d_6) δ

(ppm): 12.37 (brs, 1H), 8.49 (s, 1H), 7.16 (m, 1H), 6.99-7.01 (m, 1H), 6.88-6.93 (m, 2H), 4.13 (s, 2H), 2.77 (s, 3H), 2.47 (s, 3H), 2.23 (s, 3H). ^{13}C NMR (75 MHz, DMSO-d_6) δ (ppm): 163.5, 162.0, 146.4, 145.4, 145.0, 138.2, 137.8, 128.5, 128.3, 127.0, 124.9, 119.1, 101.9, 32.6, 23.7, 20.9, 13.7. IR ν_{max} (neat): 3391, 2941, 1672, 1615, 1548, 1521, 1486, 1374, 1231, 1193, 1143, 982, 785, 732. HRMS (ESI+): *m/z* [*M*+H]$^+$ calcd. for $C_{17}H_{18}N_3O_2^+$, 296.1394; found, 296.1394 (error 0 ppm).

5,7-dimethyl-6-(2-methylbenzyl)pyrazolo[1,5-a]pyrimidine-3-carboxylic acid (3g).: Yield: 96%. White solid. M.P. >300 °C. ^{1}H NMR (300 MHz, DMSO-d_6) δ (ppm): 12.60 (brs, 1H), 8.49 (s, 1H), 7.22-7.25 (m, 1H), 7.11 (m, 1H), 6.99 (m, 1H), 6.49-6.52 (m, 1H), 4.05 (s, 2H), 2.68 (s, 3H), 2.43 (s, 3H), 2.40 (s, 3H). ^{13}C NMR (75 MHz, DMSO-d_6) δ (ppm): 163.8, 161.9, 146.4, 145.5, 145.2, 136.2, 136.1, 130.0, 126.2.126.1, 125.8, 118.3, 102.6, 30.0, 23.2, 19.3, 13.5. IR ν_{max} (neat): 3479, 3020, 1654, 1618, 1551, 1532, 1373, 1196, 1137, 981, 845, 789, 741. HRMS (ESI−): *m/z* [*M*-H]$^-$ calcd. for $C_{17}H_{16}N_3O_2^-$, 294.1248; found, 294.1237 (error 3.74 ppm).

6-(4-isopropylbenzyl)-5,7-dimethylpyrazolo[1,5-a]pyrimidine-3-carboxylic acid (3h).: Yield: 95%. White solid. M.P. 210.3-211.9 °C. ^{1}H NMR (300 MHz, DMSO-d_6) δ (ppm): 12.61 (brs, 1H), 8.48 (s, 1H), 7.13 (d, J = 7.9 Hz, 2H), 7.01 (d, J = 7.9 Hz, 2H), 4.12 (s, 2H), 2.76-2.85 (m, 4H), 2.47 (s, 3H), 1.13 (d, J = 6.8 Hz, 6H). ^{13}C NMR (75 MHz, DMSO-d_6) δ (ppm): 163.8, 161.8, 146.4, 146.3, 145.3, 144.9, 135.5, 127.7, 126.5, 119.1, 102.6, 32.9, 32.2, 23.8, 23.6, 13.7. IR ν_{max} (neat): 3464, 2957, 1683, 1619, 1548, 1523, 1377, 1364, 1299, 1192, 1144, 849, 787, 736. HRMS (ESI+): *m/z* [2*M*+Na]$^+$ calcd. for $C_{38}H_{42}N_6O_4Na^+$, 669.3160; found, 669.3168 (error −1.23 ppm).

6-(4-methoxybenzyl)-5,7-dimethylpyrazolo[1,5-a]pyrimidine-3-carboxylic acid (3i).: Yield: 91%. White solid. M.P. 213.2-214.8 °C. ^{1}H NMR (300 MHz, DMSO-d_6) δ (ppm): 12.25 (brs, 1H), 8.49 (s, 1H), 7.03 (d, J = 8.5 Hz, 2H), 6.83 (d, J = 8.5 Hz, 2H), 4.10 (s, 2H), 3.70 (s, 3H), 2.77 (s, 3H), 2.47 (s, 3H). ^{13}C NMR (75 MHz, DMSO-d_6) δ (ppm): 163.3, 162.0, 157.8, 146.4, 145.4, 144.9, 130.0, 128.8, 119.5, 114.0, 101.7, 55.0, 31.8, 23.6, 13.7. IR ν_{max} (neat): 2937, 1661, 1611, 1548, 1511, 1426, 1246, 1190, 1021, 844, 785, 744. HRMS (ESI+): *m/z* [*M*+H]$^+$ calcd. for $C_{17}H_{18}N_3O_3^+$, 312.1343; found, 312.1348 (error −1.70 ppm).

6-(4-fluorobenzyl)-5,7-dimethylpyrazolo[1,5-a]pyrimidine-3-carboxylic acid (3j).: Yield: 96%. White solid. M.P. 201.0-202.5 °C. ^{1}H NMR (300 MHz, DMSO-d_6) δ (ppm): 8.48 (s, 1H), 7.06-7.18 (m, 4H), 4.16 (s, 2H), 2.77 (s, 3H), 2.46 (s, 3H). ^{13}C NMR (75 MHz, DMSO-d_6) δ (ppm): 163.8, 161.6, 160.7 (d, J = 240.8 Hz), 146.4, 145.3, 145.0, 134.4 (d, J = 2.8 Hz), 129.6 (d, J = 7.8 Hz), 118.8, 115.2 (d, J = 21.0 Hz), 102.7, 31.8, 23.6, 13.7. ^{19}F NMR (282 MHz, DMSO-d_6) δ (ppm): −116.7. IR ν_{max} (neat): 3063, 2585, 1659, 1615, 1550, 1509, 1385, 1362, 1249, 1196, 945, 852, 786, 770, 747. HRMS (ESI+): *m/z* [2*M*+Na]$^+$ calcd. for $C_{32}H_{28}F_2N_6O_4Na^+$, 621.2032; found, 621.2032 (error 0 ppm).

6-(4-chlorobenzyl)-5,7-dimethylpyrazolo[1,5-a]pyrimidine-3-carboxylic acid (3k).: Yield: 95%. White solid. M.P. >300 °C. ^{1}H NMR (300 MHz, DMSO-d_6) δ (ppm): 12.52 (brs, 1H), 8.49 (s, 1H), 7.33 (d, J = 8.3 Hz, 2H), 7.16 (d, J = 8.3 Hz, 2H), 4.18 (s,

2H), 2.77 (s, 3H), 2.46 (s, 3H). ^{13}C NMR (75 MHz, DMSO-d_6) δ (ppm): 163.7, 161.6, 146.5, 145.4, 145.2, 137.4, 130.9, 129.7, 128.5, 118.5, 102.7, 32.0, 23.6, 13.7. IR ν_{max} (neat): 3228, 1615, 1549, 1525, 1386, 1373, 1247, 1189, 1093, 1013, 908, 848, 797, 744. HRMS (ESI−): *m/z* [*M*-H]$^-$ calcd. for $C_{16}H_{13}ClN_3O_2^-$, 314.0702; found, 314.0691 (error 3.44 ppm).

5,7-dimethyl-6-(4-(trifluoromethyl)benzyl)pyrazolo[1,5-a]pyrimidine-3-carboxylic acid (3l).: Yield: 90%. White solid. M.P. >300 °C. ^{1}H NMR (300 MHz, DMSO-d_6) δ (ppm): 8.46 (s, 1H), 7.63 (d, *J* = 7.8 Hz, 2H), 7.36 (d, *J* = 7.8 Hz, 2H), 4.30 (s, 2H), 2.77 (s, 3H), 2.47 (s, 3H). ^{13}C NMR (75 MHz, DMSO-d_6) δ (ppm): 161.2, 146.5, 145.2, 143.5, 128.6, 127.0 (q, *J* = 31.3 Hz), 125.4 (q, *J* = 3.6 Hz), 124.2 (q, *J* = 270.1 Hz), 117.8, 32.5, 23.6, 13.7. ^{19}F NMR (282 MHz, DMSO-d_6) δ (ppm): −60.8. IR ν_{max} (neat): 3475, 1615, 1551, 1407, 1375, 1328, 1186, 1109, 1067, 902, 808. HRMS (ESI−): *m/z* [*M*-H]$^-$ calcd. for $C_{17}H_{13}F_3N_3O_2^-$, 348.0965; found, 348.0964 (error 0.39 ppm).

5-ethyl-7-methyl-6-(4-methylbenzyl)pyrazolo[1,5-a]pyrimidine-3-carboxylic acid (3m).: Yield: 91%. White solid. M.P. >300 °C. ^{1}H NMR (300 MHz, DMSO-d_6) δ (ppm): 8.27 (s, 1H), 7.07 (d, *J* = 7.5 Hz, 2H), 6.95 (d, *J* = 7.5 Hz, 2H), 4.10 (s, 2H), 3.19 (q, *J* = 7.2 Hz, 2H), 2.43 (s, 3H), 2.24 (s, 3H), 1.14 (t, *J* = 7.2 Hz, 3H). ^{13}C NMR (75 MHz, DMSO-d_6) δ (ppm): 148.4, 146.4, 144.5, 135.8, 135.2, 129.1, 127.5, 116.5, 31.8, 23.4, 20.5, 11.0. IR ν_{max} (neat): 3374, 2936, 1613, 1544, 1514, 1408, 1389, 1308, 1189, 808, 772. HRMS (ESI+): *m/z* [2*M*+Na]$^+$ calcd. for $C_{36}H_{38}N_6O_4Na^+$, 641.2847; found, 641.2847 (error 0 ppm).

5,7-diethyl-6-(4-methylbenzyl)pyrazolo[1,5-a]pyrimidine-3-carboxylic acid (3n).: Yield: 80%. Faint yellow solid. M.P. 158.1-160.5 °C. ^{1}H NMR (300 MHz, DMSO-d_6) δ (ppm): 12.13 (brs, 1H), 8.51 (s, 1H), 7.08 (d, *J* = 7.7 Hz, 2H), 6.97 (d, *J* = 7.7 Hz, 2H), 4.15 (s, 2H), 3.19 (q, *J* = 7.1 Hz, 2H), 2.75 (q, *J* = 7.3 Hz, 2H), 2.24 (s, 3H), 1.12-1.17 (m, 6H). ^{13}C NMR (75 MHz, DMSO-d_6) δ (ppm): 166.1, 163.2, 149.3, 146.6, 145.8, 135.7, 135.3, 129.2, 127.6, 117.8, 101.7, 31.2, 28.4, 20.7, 20.5, 11.8, 10.9. IR ν_{max} (neat): 3451, 2983, 2939, 1666, 1617, 1543, 1372, 1236, 1193, 1148, 787, 736. HRMS (ESI+): *m/z* [*M*+H]$^+$ calcd. for $C_{19}H_{22}N_3O_2^+$, 324.1707; found, 324.1714 (error −2.30 ppm).

4.1.4 General Procedure for the Synthesis of tert-butyl 4-phenylpiperazine-1-carboxylates (5a-k).—

A mixture of N-Boc piperazine (5.0 mmol, 1.0 eq.) and substituted bromo benzenes **4** (5.5 mmol, 1.1 eq.) in the presence of palladium acetate (0.5 mmol, 0.1 eq.), 2-Dicyclohexylphosphino-2',4',6'-triisopropylbiphenyl (1.0 mmol, 0.2 eq.) and potassium t-butoxide (6.0 mmol, 1.2 eq.) in dioxane (15 ml) was stirred in at 90 °C for 10 h. The reaction mixture was allowed to cool to room temperature, and 100 ml ethyl acetate and 100 ml water were added. The thus-obtained mixture was filtered through a celite pad. The organic layer was collected, and the aqueous phase was extracted with 50 mL EtOAc. The combined organic phases were dried over anhydrous Na_2SO_4 and concentrated *in vacuo*. The residues were purified by column chromatography (silica gel, petroleum ether (b.p. 60-90 °C)/ethyl acetate, 100:1 to 20:1) to afford the intermediates.

tert-Butyl 4-phenylpiperazine-1-carboxylate (5a).: Yield: 40%. Light brown solid. M.P. 68.0-69.1 °C. ^{1}H NMR (300 MHz, DMSO-d_6) δ (ppm): 7.19-7.24 (m, 2H), 6.92-6.95 (m, 2H), 6.80 (t, J = 7.2 Hz, 1H), 3.43-3.45 (m, 4H), 3.05-3.08 (m, 4H), 1.42 (s, 9H). ^{13}C NMR (75 MHz, DMSO-d_6) δ (ppm): 153.8, 150.9, 128.9, 119.3, 116.0, 78.9, 48.4, 42.8 (br), 28.0. IR ν_{max} (neat): 2979, 2929, 2859, 1684, 1597, 1427, 1389, 1364, 1235, 1156, 753, 689. HRMS (ESI+): m/z [M+H]$^{+}$ calcd. for $C_{15}H_{23}N_2O_2^{+}$, 263.1754; found, 263.1754 (error 0 ppm).

tert-Butyl 4-(3-(trifluoromethyl)phenyl)piperazine-1-carboxylate (5b).: Yield: 37%. Light brown solid. M.P. 45.3-47.6 °C. ^{1}H NMR (300 MHz, DMSO-d_6) δ (ppm): 7.39-7.41 (m, J = 7.9 Hz, 1H), 7.17-7.22 (m, 2H), 7.06-7.09 (m, 1H), 3.44-3.46 (m, 4H), 3.18-3.20 (m, 4H), 1.42 (s, 9H). ^{13}C NMR (75 MHz, DMSO-d_6) δ (ppm): 153.8, 151.1, 129.9 (q, J = 30.8 Hz), 129.8, 124.3 (q, J = 270.7 Hz), 119.1, 114.9 (q, J = 3.7 Hz), 111.3 (q, J = 3.7 Hz), 78.9, 47.6, 43.0 (br), 28.0. ^{19}F NMR (282 MHz, DMSO-d_6) δ (ppm): −61.1. IR ν_{max} (neat): 2979, 2933, 2828, 1684, 1607, 1420, 1389, 1362, 1234, 1153, 1109, 942, 857, 782, 691. HRMS (ESI+): m/z [M+H]$^{+}$ calcd. for $C_{16}H_{22}F_3N_2O_2^{+}$, 331.1628; found, 331.1628 (error 0 ppm).

tert-Butyl 4-(2-(trifluoromethyl)phenyl)piperazine-1-carboxylate (5c).: Yield: 51%. White solid. M.P. 46.8-48.5 °C. ^{1}H NMR (300 MHz, DMSO-d_6) δ (ppm): 7.62-7.67 (m, 2H), 7.54-7.56 (m, 1H), 7.32-7.37 (m, 1H), 3.43 (br, 4H), 2.78-2.81 (m, 4H), 1.42 (s, 9H). ^{13}C NMR (125 MHz, DMSO-d_6) δ (ppm): 153.8, 152.0, 133.6, 126.8 (q, J = 5.3 Hz), 125.7 (q, J = 27.7 Hz), 125.5, 124.7, 124.0 (q, J = 271.5 Hz), 78.9, 52.9, 44.1 (br), 43.3 (br), 28.0. ^{19}F NMR (282 MHz, DMSO-d_6) δ (ppm): −58.8. IR ν_{max} (neat): 2979, 2858, 1682, 1424, 1388, 1366, 1311, 1248, 1123, 780, 767. HRMS (ESI+): m/z [M+Na]$^{+}$ calcd. for $C_{16}H_{21}F_3N_2O_2Na^{+}$, 353.1447; found, 353.1442 (error 1.51 ppm).

tert-Butyl 4-(4-(trifluoromethyl)phenyl)piperazine-1-carboxylate (5d).: Yield: 63%. Light brown solid. M.P. 125.9-127.0 °C. ^{1}H NMR (300 MHz, DMSO-d_6) δ (ppm): 7.50 (d, J = 8.7 Hz, 2H), 7.05 (d, J = 8.7 Hz, 2H), 3.43-3.47 (m, 4H), 3.23-3.27 (m, 4H), 1.41 (s, 9H). ^{13}C NMR (75 MHz, DMSO-d_6) δ (ppm): 153.9, 153.1, 126.1 (q, J = 3.5 Hz), 124.9 (q, J = 268.6 Hz), 118.1 (q, J = 31.8 Hz), 114.5, 79.1, 46.9, 42.8 (br), 28.0. ^{19}F NMR (282 MHz, DMSO-d_6) δ (ppm): −59.5. IR ν_{max} (neat): 3001, 2931, 2820, 1672, 1614, 1418, 1392, 1367, 1326, 1232, 1137, 1107, 831, 632. HRMS (ESI+): m/z [M+H]$^{+}$ calcd. for $C_{16}H_{22}F_3N_2O_2^{+}$, 331.1628; found, 331.1623 (error 1.47 ppm).

tert-Butyl 4-(3-fluorophenyl)piperazine-1-carboxylate (5e).: Yield: 48%. White solid. M.P. 44.0-45.7 °C. ^{1}H NMR (300 MHz, DMSO-d_6) δ (ppm): 7.17-7.25 (m, 1H), 6.71-6.76 (m, 2H), 6.53-6.58 (m, 1H), 3.42-3.43 (m, 4H), 3.11-3.14 (m, 4H), 1.41 (s, 9H). ^{13}C NMR (75 MHz, DMSO-d_6) δ (ppm): 163.1 (d, J = 239.0 Hz), 153.8, 152.5 (d, J = 10.0 Hz), 130.3 (d, J = 10.0 Hz), 111.2, 104.9 (d, J = 21.2 Hz), 102.1 (d, J = 25.0 Hz), 78.9, 47.6, 42.9 (br), 28.0. ^{19}F NMR (282 MHz, DMSO-d_6) δ (ppm): −112.3. IR ν_{max} (neat): 2981, 2859, 1682, 1609, 1581, 1497, 1424, 1390, 1364, 1243, 1157, 1124, 996, 967, 759, 682. HRMS (ESI+): m/z [M+H]$^{+}$ calcd. for $C_{15}H_{22}FN_2O_2^{+}$, 281.1660; found, 281.1660 (error 0 ppm).

tert-Butyl 4-(3-chlorophenyl)piperazine-1-carboxylate (5f).: Yield: 51%. White solid. M.P. 64.6-65.8 °C. ^{1}H NMR (500 MHz, DMSO-d_6) δ (ppm): 7.19-7.22 (m, 1H), 6.94-6.95

(m, 1H), 6.87-6.89 (m, 1H), 6.78-6.80 (m, 1H), 3.42-3.44 (m, 4H), 3.11-3.13 (m, 4H), 1.41 (s, 9H). ^{13}C NMR (125 MHz, DMSO-d_6) δ (ppm): 153.8, 152.1, 133.8, 130.4, 118.5, 115.0, 114.1, 79.0, 47.7, 43.2 (br), 28.0. IR ν_{max} (neat): 2976, 2861, 1679, 1592, 1424, 1391, 1364, 1235, 1158, 1124, 933, 760, 679. HRMS (ESI+): *m/z* [*M*+H]$^+$ calcd. for $C_{15}H_{22}ClN_2O_2^+$, 297.1364; found, 297.1365 (error −0.23 ppm).

tert-Butyl 4-(3-(difluoromethyl)phenyl)piperazine-1-carboxylate (5g).: Yield: 51%. Light brown solid. M.P. 61.1-62.8 °C. ^{1}H NMR (300 MHz, DMSO-d_6) δ (ppm): 7.32-7.37 (m, 1H), 7.10 (m, 2H), 6.97-6.99 (m, 1H), 6.91 (t, J = 56.0 Hz, 1H), 3.44-3.46 (m, 4H), 3.13-3.16 (m, 4H), 1.42 (s, 9H). ^{13}C NMR (75 MHz, DMSO-d_6) δ (ppm): 153.8, 151.0, 134.9 (t, J = 21.6 Hz), 129.5, 117.9, 115.9 (t, J =5.8 Hz), 115.2 (t, J = 234.6 Hz), 112.6 (t, J = 6.3 Hz), 79.0, 47.9, 43.0 (br), 28.0. ^{19}F NMR (282 MHz, DMSO-d_6) δ (ppm): −112.3. IR ν_{max} (neat): 2977, 2862, 1682, 1425, 1388, 1364, 1244, 1165, 1129, 1018, 950, 867, 801, 751. HRMS (ESI+): *m/z* [*M*+H]$^+$ calcd. for $C_{16}H_{23}F_2N_2O_2^+$, 313.1722; found, 313.1720 (error 0.67 ppm).

tert-Butyl 4-(3-cyanophenyl)piperazine-1-carboxylate (5h).: Yield: 28%. White solid. M.P. 130.1-131.2 °C. ^{1}H NMR (300 MHz, DMSO-d_6) δ (ppm): 7.33-7.41 (m, 2H), 7.25-7.28 (m, 1H), 7.15-7.18 (m, 1H), 3.42-3.44 (m, 4H), 3.17-3.20 (m, 4H), 1.41 (s, 9H). ^{13}C NMR (75 MHz, DMSO-d_6) δ (ppm): 153.8, 150.9, 130.1, 121.9, 120.0, 119.2, 118.0, 112.0, 79.0, 47.3, 42.8 (br), 28.0. IR ν_{max} (neat): 2979, 2866, 2222, 1674, 1598, 1573, 1425, 1393, 1364, 1241, 1157, 1123, 992, 952, 783, 683. HRMS (ESI+): *m/z* [*M*+H]$^+$ calcd. for $C_{16}H_{22}N_3O_2^+$, 288.1707; found, 288.1709 (error −0.86 ppm).

tert-Butyl 4-(m-tolyl)piperazine-1-carboxylate (5i).: Yield: 51%. Light brown solid. M.P. 66.3-67.1 °C. ^{1}H NMR (300 MHz, DMSO-d_6) δ (ppm): 7.07-7.12 (m, 1H), 6.71-6.75 (m, 2H), 6.61-6.63 (m, 1H), 3.42-3.45 (m, 4H), 3.03-3.06 (m, 4H), 2.25 (s, 3H), 1.42 (s, 9H). ^{13}C NMR (75 MHz, DMSO-d_6) δ (ppm): 153.8, 150.9, 137.9, 128.7, 120.1, 116.6, 113.1, 78.8, 48.4, 43.2 (br), 28.0, 21.3. IR ν_{max} (neat): 2973, 2917, 2820, 1694, 1599, 1423, 1385, 1363, 1421, 1157, 1118, 948, 767, 688. HRMS (ESI+): *m/z* [*M*+H]$^+$ calcd. for $C_{16}H_{25}N_2O_2^+$, 277.1911; found, 277.1911 (error 0 ppm).

tert-Butyl 4-(3-isopropylphenyl)piperazine-1-carboxylate (5j).: Yield: 72%. White solid. M.P. 39.7-40.5 °C. ^{1}H NMR (300 MHz, DMSO-d_6) δ (ppm): 7.10-7.15 (m, 1H), 6.81 (s, 1H), 6.68-6.75 (m, 2H), 3.43-3.45 (m, 4H), 3.04-3.07 (m, 4H), 2.81 (hept, J = 6.8 Hz, 1H), 1.42 (s, 9H), 1.18 (d, J = 6.8 Hz, 6H). ^{13}C NMR (75 MHz, DMSO-d_6) δ (ppm): 153.8, 151.0, 149.1, 128.7, 117.4, 114.3, 113.5, 78.8, 48.6, 43.1 (br), 33.7, 28.0, 23.9. IR ν_{max} (neat): 2958, 2861, 2822, 1687, 1605, 1421, 1364, 1339, 1213, 1160, 1121, 953, 778, 703. HRMS (ESI+): *m/z* [*M*+H]$^+$ calcd. for $C_{18}H_{29}N_2O_2^+$, 305.2224; found, 305.2224 (error 0 ppm).

tert-Butyl 4-(3-methoxyphenyl)piperazine-1-carboxylate (5k).: Yield: 36%. White solid. M.P. 59.8-61.8 °C. ^{1}H NMR (300 MHz, DMSO-d_6) δ (ppm): 7.09-7.14 (m, 1H), 6.38-6.53 (m, 3H), 3.71 (s, 3H), 3.42-3.45 (m,4H), 3.05-3.09 (m, 4H), 1.42 (s, 9H). ^{13}C NMR (75 MHz, DMSO-d_6) δ (ppm): 160.2, 153.8, 152.2, 129.6, 108.5, 104.6, 102.0, 78.9, 54.8, 48.3, 43.1 (br), 28.0. IR ν_{max} (neat): 2973, 2923, 2873, 1690, 1585, 1417, 1369, 1245, 1162, 995,

945, 819, 760, 684. HRMS (ESI+): *m/z* [*M*+H]$^+$ calcd. for $C_{16}H_{25}N_2O_3^+$, 293.1860; found, 293.1858 (error 0.58 ppm).

4.1.5 General Procedure for the Synthesis of Pyrazolo[1,5-*a*]pyrimidine-3-carboxamides (21-48).—

The Boc protected 4-phenylpiperazines (1.5 mmol) were dissolved in 8 ml of 4M HCl/EtOAc and the reaction mixture was stirred at room temperature for 2 h. Then the reaction mixture was evaporated *in vacuo* to give the crude piperazine hydrochlorides as near white solid, which was subjected to the next reaction without further purification.

To a mixture of pyrazolo[1,5-*a*]pyrimidine-3-carboxylic acids (1.0 mmol, 1.0 eq.) and amine (1.1 mmol, 1.1 eq.) in DMF (8 mL) was added HATU (1.5 mmol, 1.5 eq.), followed by DIEA (3.0 mmol, 3.0 eq.). The mixture was stirred at room temperature overnight and then diluted with 80 mL EtOAc and washed with 30 mL saturated aqueous NaCl. The organic layer was dried over anhydrous Na_2SO_4 and concentrated *in vacuo*. The residue was purified by column chromatography (silica gel, petroleum ether (b.p.60-90°C)/ethyl acetate, 20:1 to 1:3) to afford the desired compounds as solid.

(5,7-diethyl-6-(4-methylbenzyl)pyrazolo[1,5-a]pyrimidin-3-yl)(4-(3-(trifluoromethyl)phenyl)piperazin-1-yl)methanone (21).: Yield: 87%. White solid. M.P. 64.4-66.0 °C. ^{1}H NMR (300 MHz, DMSO-d_6) δ (ppm): 8.40 (s, 1H), 7.40-7.45 (m, 1H), 7.21-7.25 (m, 2H), 7.08-7.10 (m, 3H), 6.98-7.01 (m, 2H), 4.15 (s, 2H), 3.78 (s, 4H), 3.34 (s, 4H), 3.21 (q, *J* = 7.4 Hz, 2H), 2.75 (q, *J* = 7.3 Hz, 2H), 2.24 (s, 3H), 1.13-1.20 (m, 6H). ^{13}C NMR (75 MHz, DMSO-d_6) δ (ppm): 164.7, 162.7, 151.1, 148.9, 145.8, 142.7, 135.7, 135.3, 130.0, 129.9 (q, *J* = 30.8 Hz), 129.2, 127.6, 124.3 (q, *J* = 270.8 Hz), 119.0, 117.0, 114.9 (q, *J* = 3.6 Hz), 111.2 (q, *J* = 3.7 Hz), 104.8, 48.2 (br), 31.2, 28.3, 20.7, 20.5, 11.5, 10.9. ^{19}F NMR (282 MHz, DMSO-d_6) δ (ppm): −61.1. IR ν_{max} (neat): 2935, 1732, 1610, 1544, 1514, 1449, 1350, 1306, 1232, 1158, 1116, 994, 944, 844, 786, 695. HRMS (ESI+): *m/z* [*M*+H]$^+$ calcd. for $C_{30}H_{33}F_3N_5O^+$, 536.2632; found, 536.2632 (error 0 ppm).

(5-ethyl-7-methyl-6-(4-methylbenzyl)pyrazolo[1,5-a]pyrimidin-3-yl)(4-(3-(trifluoromethyl)phenyl)piperazin-1-yl)methanone (22).: Yield: 84%. White solid. M.P. 62.3-63.7 °C. ^{1}H NMR (300 MHz, DMSO-d_6) δ (ppm): 8.39 (s, 1H), 7.39-7.44 (m, 1H), 7.21-7.24 (m, 2H), 7.07-7.10 (m, 3H), 6.98-7.01 (m, 2H), 4.12 (s, 2H), 3.75 (s, 4H), 3.34 (m, 4H), 3.21 (q, *J* = 7.2 Hz, 2H), 2.43 (s, 3H), 2.23 (s, 3H), 1.18 (t, *J* = 7.2 Hz, 3H). ^{13}C NMR (75 MHz, DMSO-d_6) δ (ppm): 162.6, 161.1, 151.0, 148.8, 145.4, 142.8, 135.5, 135.3, 130.1, 129.9 (q, *J* = 30.8 Hz), 129.2, 127.6, 124.3 (q, *J* = 270.7 Hz), 118.9, 117.4, 114.8 (q, *J* = 3.6 Hz), 111.2 (q, *J* = 3.7 Hz), 104.6, 48.0 (br), 31.8, 23.7, 20.6, 20.4, 10.9. ^{19}F NMR (282 MHz, DMSO-d_6) δ (ppm): −61.1. IR ν_{max} (neat): 2938, 1613, 1547, 1514, 1449, 1391, 1318, 1306, 1232, 1159, 1116, 993, 944, 857, 782, 696. HRMS (ESI+): *m/z* [*M*+Na]$^+$ calcd. for $C_{29}H_{30}F_3N_5ONa^+$, 544.2295; found, 544.2292 (error 0.49 ppm).

(6-benzylpyrazolo[1,5-a]pyrimidin-3-yl)(4-phenylpiperazin-1-yl)methanone (23).: Yield: 85%. White solid. M.P. 120.7-122.8 °C. ^{1}H NMR (300 MHz, DMSO-d_6) δ (ppm): 9.18 (s, 1H), 8.66 (m, 1H), 8.41 (s, 1H), 7.29-7.38 (m, 4H), 7.18-7.23 (m, 3H), 6.92-6.95 (m, 2H), 6.77-6.81 (m, 1H), 4.06 (s, 2H), 3.70 (brs, 4H), 3.17 (brs, 4H). ^{13}C

NMR (75 MHz, DMSO-d_6) δ (ppm): 162.1, 153.5, 150.8, 146.0, 143.0, 139.6, 134.5, 128.9, 128.7, 126.5, 122.9, 119.3, 115.9, 105.4, 48.8, 34.5. IR ν_{max} (neat): 3059, 2919, 2853, 1669, 1627, 1494, 1384, 1231, 1205, 1007, 842, 761, 698. HRMS (ESI+): *m/z* $[2M+H]^+$ calcd. for $C_{48}H_{47}N_{10}O_2^+$, 795.3878; found, 795.3876 (error 0.25 ppm).

(6-(4-fluorobenzyl)-5,7-dimethylpyrazolo[1,5-a]pyrimidin-3-yl)(4-(3-(trifluoromethyl)phenyl)piperazin-1-yl)methanone (24).: Yield: 69%. White solid. M.P. 60.6-62.2 °C. ^{1}H NMR (300 MHz, DMSO-d_6) δ (ppm): 8.39 (s, 1H), 7.40-7.45 (m, 1H), 7.17-7.25 (m, 4H), 7.07-7.13 (m, 3H), 4.17 (s, 2H), 3.75 (s, 4H), 3.34 (s, 4H), 2.79 (s, 3H), 2.45 (s, 3H). ^{13}C NMR (75 MHz, DMSO-d_6) δ (ppm): 162.6, 160.8 (d, J = 240.8 Hz), 160.6, 151.0, 145.4, 144.7, 142.7, 134.5 (d, J = 2.8 Hz), 130.0, 129.9 (q, J = 30.7 Hz), 129.7, 129.6, 124.3 (q, J = 270.8 Hz), 118.9, 118.1, 115.4, 115.1, 114.8 (q, J = 3.7 Hz), 111. 2 (q, J = 3.7 Hz), 104.6, 48.0 (br), 31.8, 23.7, 13.6. ^{19}F NMR (282 MHz, DMSO-d_6) δ (ppm): −61.1, −116.8. IR ν_{max} (neat): 2916, 1731, 1614, 1548, 1507, 1429, 1352, 1318, 1306, 1220, 1156, 1115, 989, 943, 845, 784, 695. HRMS (ESI+): *m/z* $[M+H]^+$ calcd. for $C_{27}H_{26}F_4N_5O^+$, 512.2068; found, 512.2062 (error 1.17 ppm).

(6-(4-chlorobenzyl)-5,7-dimethylpyrazolo[1,5-a]pyrimidin-3-yl)(4-(3-(trifluoromethyl)phenyl)piperazin-1-yl)methanone (25).: Yield: 67%. White solid. M.P. 180.1-181.8 °C. ^{1}H NMR (300 MHz, DMSO-d_6) δ (ppm): 8.39 (s 1H), 7.40-7.45 (m, 1H), 7.32-7.35 (m, 2H), 7.17-7.26 (m, 4H), 7.07-7.09 (m, 1H), 4.18 (s, 2H), 3.74 (s, 4H), 3.35 (s, 4H), 2.78 (s, 3H), 2.44 (s, 3H). ^{13}C NMR (75 MHz, DMSO-d_6) δ (ppm): 162.6, 160.6, 151.1, 145.4, 144.9, 142.8, 137.6, 130.9, 130.0, 129.9 (q, J = 31.0 Hz), 129.7, 128.5, 124.4 (q, J = 270.7 Hz), 119.0, 117.9, 114.8 (q, J = 3.6 Hz), 111.3 (q, J = 3.6 Hz), 104.7, 48.1 (br), 32.0, 23.8, 13.7. ^{19}F NMR (282 MHz, DMSO-d_6) δ (ppm): −61.1. IR ν_{max} (neat): 3103, 2816, 1608, 1543, 1447, 1431, 1382, 1352, 1319, 1157, 1100, 992, 942, 845, 784, 772. HRMS (ESI+): *m/z* $[M+H]^+$ calcd. for $C_{27}H_{26}ClF_3N_5O^+$, 528.1773; found, 528.1762 (error 1.98 ppm).

(6-(4-methoxybenzyl)-5,7-dimethylpyrazolo[1,5-a]pyrimidin-3-yl)(4-(3-(trifluoromethyl)phenyl)piperazin-1-yl)methanone (26).: Yield: 90%. White solid. M.P. 53.7-55.5 °C. ^{1}H NMR (300 MHz, DMSO-d_6) δ (ppm): 8.38 (s, 1H), 7.39-7.44 (m, 1H), 7.21-7.24 (m, 2H), 7.03-7.08 (m, 3H), 6.82-6.85 (m, 2H), 4.08 (s, 2H), 3.74 (s, 4H), 3.69 (s, 3H), 3.34 (s, 4H), 2.78 (s, 3H), 2.45 (s, 3H). ^{13}C NMR (75 MHz, DMSO-d_6) δ (ppm): 162.7, 160.7, 157.8, 151.1, 145.4, 144.5, 142.7, 130.1, 130.0, 129.9 (q, J = 30.8 Hz), 128.8, 124.4 (q, J = 270.8 Hz), 119.0, 118.7, 114.9 (q, J = 3.7 Hz), 114.1, 111.3 (q, J = 3.7 Hz), 104.6, 55.0, 48.1 (br), 31.8, 23.7, 13.7. ^{19}F NMR (282 MHz, DMSO-d_6) δ (ppm): −61.1. IR ν_{max} (neat): 1613, 1583, 1510, 1445, 1383, 1312, 1245, 1113, 1025, 990, 839, 790, 699. HRMS (ESI+): *m/z* $[M+H]^+$ calcd. for $C_{28}H_{29}F_3N_5O_2^+$, 524.2268; found, 524.2264 (error 0.73 ppm).

(5,7-dimethyl-6-(3-methylbenzyl)pyrazolo[1,5-a]pyrimidin-3-yl)(4-(3-(trifluoromethyl)phenyl)piperazin-1-yl)methanone (27).: Yield: 95%. White solid. M.P. 62.5-65.0 °C. ^{1}H NMR (300 MHz, DMSO-d_6) δ (ppm): 8.39 (s, 1H), 7.39-7.45 (m, 1H), 7.14-7.25 (m, 3H), 7.07-7.09 (m, 1H), 6.97-7.02 (m, 2H),

6.89-6.92 (m, 1H), 4.13 (s, 2H), 3.74 (s, 4H), 3.34 (s, 4H), 2.78 (s, 3H), 2.45 (s, 3H), 2.24 (s, 3H). ^{13}C NMR (75 MHz, DMSO-d_6) δ (ppm): 162.6, 160.7, 151.1, 145.3, 144.7, 142.7, 138.3, 137.8, 130.0, 129.9 (q, J = 30.8 Hz), 128.5, 128.4, 127.0, 124.8, 124.3 (q, J = 270.6 Hz), 119.0, 118.3, 114.8 (q, J = 3.4 Hz), 111.3 (q, J = 3.5 Hz), 104.6, 48.1 (br), 32.6, 23.8, 21.0, 13.7. ^{19}F NMR (282 MHz, DMSO-d_6) δ (ppm): −61.1. IR ν_{max} (neat): 2925, 1613, 1550, 1446, 1383, 1315, 1160, 1114, 1025, 990, 838, 791, 771, 734, 702. HRMS (ESI+): *m/z* [*M*+Na]$^+$ calcd. for $C_{28}H_{28}F_3N_5ONa^+$, 530.2138; found, 530.2135 (error 0.59 ppm).

(5,7-dimethyl-6-(2-methylbenzyl)pyrazolo[1,5-a]pyrimidin-3-yl)(4-(3-(trifluoromethyl)phenyl)piperazin-1-yl)methanone (28).: Yield: 84%. White solid. M.P. 91.1- 93.5 °C. ^{1}H NMR (300 MHz, DMSO-d_6) δ (ppm): 8.40 (s, 1H), 7.40-7.45 (m, 1H), 7.23-7.26 (m, 3H), 7.07-7.14 (m, 2H), 6.98-7.03 (m, 1H), 6.55-6.57 (m, 1H), 4.06 (s, 2H), 3.77 (s, 4H), 3.38 (s ,4H), 2.69 (s, 3H), 2.44 (s, 3H), 2.39 (s, 3H). ^{13}C NMR (75 MHz, DMSO-d_6) δ (ppm): 162.7, 160.8, 151.1, 145.4, 144.9, 142.9, 136.3, 136.1, 130.0, 129.9 (q, J = 30.8 Hz), 126.2, 126.2, 125.8, 124.4 (q, J = 270.9 Hz), 119.0, 117.7, 114.8 (q, J = 3.6 Hz), 111.3 (q, J = 3.6 Hz), 104.7, 48.0 (br), 30.0, 23.4, 19.4, 13.5. ^{19}F NMR (282 MHz, DMSO-d_6) δ (ppm): −61.1. IR ν_{max} (neat): 2914, 1615, 1548, 1432, 1352, 1318, 1307, 1159, 1117, 1027, 991, 944, 840, 765, 696. HRMS (ESI+): *m/z* [*M*+Na]$^+$ calcd. for $C_{28}H_{28}F_3N_5ONa^+$, 530.2138; found, 530.2130 (error 1.54 ppm).

(6-(4-isopropylbenzyl)-5,7-dimethylpyrazolo[1,5-a]pyrimidin-3-yl)(4-(3-(trifluoromethyl)phenyl)piperazin-1-yl)methanone (29).: Yield: 65%. White solid. M.P. 176.4-177.9 °C. ^{1}H NMR (300 MHz, DMSO-d_6) δ (ppm): 8.38 (s, 1H), 7.40-7.45 (m, 1H), 7.21-7.25 (m, 2H), 7.14-7.17 (m, 2H), 7.04-7.09 (m, 3H), 4.14 (s, 2H), 3.74 (s, 4H), 3.34 (s, 4H), 2.79-2.88 (m, 4H), 2.46 (s, 3H), 1.15 (d, J = 6.8 Hz, 6H). 13C NMR (75 MHz, DMSO-d_6) δ (ppm): 162.6, 160.7, 151.0, 146.3, 145.3, 144.5, 142.7, 135.6, 130.0, 129.8 (q, J = 31.1 Hz), 127.7, 126.5, 124.3 (q, J = 270.8 Hz), 118.9, 118.4, 114.8 (q, J = 3.7 Hz), 111.2 (q, J = 3.7 Hz), 104.6, 48.0 (br), 32.9, 32.2, 23.8, 13.7. ^{19}F NMR (282 MHz, DMSO-d_6) δ (ppm): −61.1. IR νmax (neat): 2959, 1614, 1541, 1447, 1428, 1376, 1351, 1235, 1156, 1118, 1026, 992, 846, 774, 691. HRMS (ESI+): *m/z* [*M*+H]$^+$ calcd. for $C_{30}H_{33}F_3N_5O^+$, 536.2632; found, 536.2631 (error 0.13 ppm).

(5,7-dimethyl-6-(4-(trifluoromethyl)benzyl)pyrazolo[1,5-a]pyrimidin-3-yl)(4-(3-(trifluoromethyl)phenyl)piperazin-1-yl)methanone (30).: Yield: 60%. White solid. M.P. 202.6- 203.6 °C. ^{1}H NMR (300 MHz, DMSO-d_6) δ (ppm): 8.40 (s, 1H), 7.63-7.66 (m, 2H), 7.38-7.45 (m, 3H), 7.21-7.26 (m, 2H), 7.07-7.10 (m, 1H), 4.31 (s, 2H), 3.75 (s, 4H), 3.35 (s, 4H), 2.80 (s, 3H), 2.45 (s, 3H). ^{13}C NMR (75 MHz, DMSO-d_6) δ (ppm): 162.5, 160.5, 151.0, 145.4, 145.0, 143.5, 142.8, 129.9, 129.8 (q, J = 30.8 Hz), 128.7, 127.0 (q, J = 31.5 Hz), 125.3 (q, J = 3.6 Hz), 124.3 (q, J = 270.7 Hz), 124.2 (q, J = 270.3 Hz), 118.9, 117.4, 114.8 (q, J = 3.7 Hz), 111.2 (q, J = 3.7 Hz), 104.7, 48.0 (br), 32.5, 23.7, 13.7. ^{19}F NMR (282 MHz, DMSO-d_6) δ (ppm): −60.8, −61.1. IR ν_{max} (neat): 2816, 1609, 1447, 1432, 1383, 1319, 1159, 1111, 1066, 1018, 993, 943, 849, 788, 691. HRMS (ESI+): *m/z* [*M*+Na]$^+$ calcd. for $C_{28}H_{25}F_6N_5ONa^+$, 584.1856; found, 584.1851 (error 0.77 ppm).

(6-ethyl-5,7-dimethylpyrazolo[1,5-a]pyrimidin-3-yl)(4-phenylpiperazin-1-yl)methanone (31).: Yield: 73%. White solid. M.P. 143.0-144.4 °C. ^{1}H NMR (300 MHz, DMSO-d_6) δ (ppm): 8.33 (s, 1H), 7.19-7.25 (m, 2H), 6.95-6.98 (m, 2H), 6.77-6.82 (m, 1H), 3.72 (brs, 4H), 3.22 (brs, 4H), 2.69-2.74 (m, 5H), 2.60 (s, 3H), 1.13 (t, J = 7.3 Hz, 3H). ^{13}C NMR (75 MHz, DMSO-d_6) δ (ppm): 162.6, 160.0, 150.9, 145.1, 143.3, 142.4, 129.0, 121.4, 119.2, 115.8, 104.4, 48.8 (br), 23.3, 20.6, 13.6, 12.9. IR ν_{max} (neat): 2966, 2923, 2864, 1617, 1596, 1542, 1429, 1370, 1227, 1191, 837, 754, 689. HRMS (ESI+): *m/z* $[2M+Na]^+$ calcd. for $C_{42}H_{50}N_{10}O_2Na^+$, 749.4010; found, 749.4010 (error 0 ppm).

(5,7-dimethyl-6-phenylpyrazolo[1,5-a]pyrimidin-3-yl)(4-phenylpiperazin-1-yl)methanone (32).: Yield: 84%. White solid. M.P. 97.0-98.5 °C. ^{1}H NMR (500 MHz, DMSO-d_6) δ (ppm): 8.43 (s, 1H), 7.53-7.56 (m, 2H), 7.48-7.50 (m, 1H), 7.38-7.40 (m, 2H), 7.21-7.24 (m, 2H), 6.96-6.98 (m, 2H), 6.80 (t, J = 7.2 Hz, 1H), 3.77 (s, 4H), 3.24-3.26 (m, 4H), 2.48 (s, 3H), 2.29 (s, 3H). ^{13}C NMR (125 MHz, DMSO-d_6) δ (ppm): 162.4, 159.2, 150.9, 145.7, 143.8, 143.0, 134.9, 134.8, 129.9, 128.9, 128.8, 128.2, 122.4, 119.2, 115.8, 104.8, 48.8, 24.6, 14.8. IR ν_{max} (neat): 3056, 2920, 2850, 1722, 1614, 1597, 1494, 1385, 1228, 839, 757, 704, 692. HRMS (ESI+): *m/z* $[2M+Na]^+$ calcd. for $C_{50}H_{50}N_{10}O_2Na^+$, 845.4010; found, 845.4010 (error 0 ppm).

(5,7-dimethyl-6-(4-methylbenzyl)pyrazolo[1,5-a]pyrimidin-3-yl)(4-(4-(trifluoromethyl)phenyl)piperazin-1-yl)methanone (33).: Yield: 92%. White solid. M.P. 76.5-78.1 °C. ^{1}H NMR (300 MHz, DMSO-d_6) δ (ppm): 8.39 (s, 1H), 7.50 (d, J = 8.6 Hz, 2H), 7.00-7.10 (m, 6H), 4.11 (s, 2H), 3.74 (s, 4H), 3.40 (s, 4H), 2.78 (s, 3H), 2.45 (s, 3H), 2.24 (s, 3H). ^{13}C NMR (75 MHz, DMSO-d_6) δ (ppm): 162.6, 160.6, 153.0, 145.3, 144.5, 142.7, 135.3, 135.2, 129.2, 127.7, 126.1 (q, J = 3.5 Hz), 124.8 (q, J = 268.7 Hz), 118.4, 118.0 (q, J = 31.8 Hz), 114.3, 104.6, 47.3 (br), 32.2, 23.7, 20.5, 13.6. ^{19}F NMR (282 MHz, DMSO-d_6) δ (ppm): −59.5. IR ν_{max} (neat): 2920, 2855, 1613, 1547, 1522, 1428, 1385, 1326, 1230, 1193, 1104, 1069, 988, 824. HRMS (ESI+): *m/z* $[M+H]^+$ calcd. for $C_{28}H_{29}F_3N_5O^+$, 508.2319; found, 508.2302 (error 3.29 ppm).

(5,7-dimethyl-6-(4-methylbenzyl)pyrazolo[1,5-a]pyrimidin-3-yl)(4-(2-(trifluoromethyl)phenyl)piperazin-1-yl)methanone (34).: Yield: 91%. White solid. M.P. 171.4-173.4 °C. ^{1}H NMR (300 MHz, DMSO-d_6) δ (ppm): 8.38 (s, 1H), 7.58-7.69 (m, 3H), 7.33-7.38 (m, 1H), 7.08 (d, J = 7.7 Hz, 2H), 7.01 (d, J = 7.7 Hz, 2H), 4.12 (s, 2H), 3.72 (s, 4H), 2.93 (s ,4H), 2.77 (s, 3H), 2.46 (s, 3H), 2.24 (s, 3H). ^{13}C NMR (75 MHz, DMSO-d_6) δ (ppm): 162.5, 160.6, 151.9, 145.2, 144.5, 142.7, 135.3, 135.2, 133.6, 129.2, 127.7, 126.8 (q, J = 5.2 Hz), 125.7 (q, J = 27.8 Hz), 125.4, 124.7, 124.0 (q, J = 271.6 Hz), 118.4, 104.7, 53.4 (br), 32.2, 23.7, 20.5, 13.6. ^{19}F NMR (282 MHz, DMSO-d_6) δ (ppm): −58.7. IR ν_{max} (neat): 2916, 2810, 1620, 1548, 1514, 1481, 1430, 1377, 1312, 1120, 1107, 1036, 1025, 988, 771. HRMS (ESI+): *m/z* $[M+H]^+$ calcd. for $C_{28}H_{29}F_3N_5O^+$, 508.2319; found, 508.2304 (error 2.89 ppm).

(4-(3-(difluoromethyl)phenyl)piperazin-1-yl)(5,7-dimethyl-6-(4-methylbenzyl)pyrazolo[1,5-a]pyrimidin-3-yl)methanone (35).: Yield: 89%. White solid. M.P. 82.3-84.3 °C. ^{1}H NMR (300 MHz, DMSO-

d$_6$) δ (ppm): 8.38 (s, 1H), 7.32-7.37 (m, 1H), 7.07-7.13 (m, 4H), 6.96-7.03 (m, 3H), 6.92 (t, *J* = 56.0 Hz, 1H), 4.12 (s, 2H), 3.74 (s, 4H), 3.30 (s, 4H), 2.78 (s, 3H), 2.45 (s, 3H), 2.24 (s, 3H). ^{13}C NMR (75 MHz, DMSO-*d*$_6$) δ (ppm): 162.6, 160.7, 150.9, 145.3, 144.5, 142.7, 135.3, 135.2, 134.8 (t, *J* = 21.7 Hz), 129.6, 129.2, 127.7, 118.4, 118.3, 117.8 (br), 115.7 (t, *J* = 5.7 Hz), 115.2 (t, *J* = 234.7 Hz), 112.5 (t, *J* = 6.3 Hz), 112.1, 104.6, 48.3 (br), 32.2, 23.7, 20.5, 13.6. ^{19}F NMR (282 MHz, DMSO-*d*$_6$) δ (ppm): −109.0. IR ν_{max} (neat): 2921, 1614, 1548, 1480, 1432, 1377, 1236, 1192, 1026, 992, 840, 792, 774, 699. HRMS (ESI+): *m/z* [*M*+Na]$^+$ calcd. for $C_{28}H_{29}F_2N_5ONa^+$, 512.2232; found, 512.2232 (error 0 ppm).

3-(4-(5,7-dimethyl-6-(4-methylbenzyl)pyrazolo[1,5-a]pyrimidine-3-carbonyl)piperazin-1-yl)benzo nitrile (36).: Yield: 94%. White solid. M.P. 83.8-85.8 °C. ^{1}H NMR (300 MHz, DMSO-*d*$_6$) δ (ppm): 8.38 (s, 1H), 7.37-7.42 (m, 2H), 7.29-7.31 (m, 1H), 7.16-7.19 (m, 1H), 7.09 (d, *J* = 7.8 Hz, 2H), 7.02 (d, *J* = 7.8 Hz, 2H), 4.13 (s, 2H), 3.72 (s, 4H), 3.34 (s, 4H), 2.78 (s, 3H), 2.45 (s, 3H), 2.25 (s, 3H). ^{13}C NMR (75 MHz, DMSO-*d*$_6$) δ (ppm): 162.6, 160.7, 150.8, 145.3, 144.6, 142.7, 135.3, 135.2, 130.2, 129.2, 127.7, 121.8, 119.9, 119.2, 118.4, 117.9, 112.0, 104.6, 47.7 (br), 32.2, 23.8, 20.5, 13.7. IR ν_{max} (neat): 2921, 2227, 1615, 1595, 1547, 1430, 1376, 1236, 1193, 1028, 991, 840, 772. HRMS (ESI+): *m/z* [*M*+H]$^+$ calcd. for $C_{28}H_{29}N_6O^+$, 465.2397; found, 465.2401 (error −0.78 ppm).

(5,7-dimethyl-6-(4-methylbenzyl)pyrazolo[1,5-a]pyrimidin-3-yl)(4-(3-fluorophenyl)piperazin-1-yl)methanone (37).: Yield: 96%. White solid. M.P. 62.0-63.4 °C. ^{1}H NMR (300 MHz, DMSO-*d*$_6$) δ (ppm): 8.38 (s, 1H), 7.17-7.25 (m, 1H), 7.09 (d, *J* = 7.8 Hz, 2H), 7.02 (d, *J* = 7.8 Hz, 2H), 6.74-6.79 (m, 2H), 6.53-6.58 (m, 1H), 4.12 (s, 2H), 3.72 (s, 4H), 3.28 (s, 4H), 2.78 (s, 3H), 2.45 (s, 3H), 2.25 (s, 3H). ^{13}C NMR (75 MHz, DMSO-*d*$_6$) δ (ppm): 163.2 (d, *J* = 238.9 Hz), 162.6, 160.7, 152.5 (d, *J* = 10.0 Hz), 145.3, 144.5, 142.7, 135.3, 135.2, 130.3 (d, *J* = 10.0 Hz), 129.2, 127.7, 118.4, 111.1, 104.9 (d, *J* = 21.2 Hz), 104.6, 102.0 (d, *J* = 25.0 Hz), 48.1 (br), 32.2, 23.7, 20.5, 13.6. ^{19}F NMR (282 MHz, DMSO-*d*$_6$) δ (ppm): −112.3. IR ν_{max} (neat): 2919, 1668, 1611, 1582, 1547, 1494, 1434, 1385, 1243, 1160, 992, 968, 834, 772. HRMS (ESI+): *m/z* [2*M*+Na]$^+$ calcd. for $C_{54}H_{56}F_2N_{10}O_2Na^+$, 937.4448; found, 937.4448 (error 0 ppm).

(4-(3-chlorophenyl)piperazin-1-yl)(5,7-dimethyl-6-(4-methylbenzyl)pyrazolo[1,5-a]pyrimidin-3-yl)methanone (38).: Yield: 70%. White solid. M.P. 70.6-72.5 °C. ^{1}H NMR (300 MHz, DMSO-*d*$_6$) δ (ppm): 8.37 (s, 1H), 7.18-7.23 (m, 1H), 7.08 (d, *J* = 7.8 Hz, 2H), 7.01 (d, *J* = 7.8 Hz, 2H), 6.89-6.96 (m, 2H), 6.77-6.80 (m, 1H), 4.11 (s, 2H), 3.72 (s, 4H), 3.28 (s, 4H), 2.78 (s, 3H), 2.45 (s, 3H), 2.24 (s, 3H). ^{13}C NMR (75 MHz, DMSO-*d*$_6$) δ (ppm): 162.5, 160.6, 152.0, 145.3, 144.5, 142.6, 135.3, 135.2, 133.8, 130.4, 129.2, 127.7, 118.4, 118.3, 114.9, 113.9, 104.6, 48.0 (br), 32.2, 23.7, 20.5, 13.6. IR ν_{max} (neat): 2916, 1618, 1589, 1550, 1479, 1429, 1383, 1192, 1025, 989, 774. HRMS (ESI+): *m/z* [*M*+H]$^+$calcd. for $C_{27}H_{29}ClN_5O^+$, 474.2055; found, 474.2058 (error −0.60 ppm).

(5,7-dimethyl-6-(4-methylbenzyl)pyrazolo[1,5-a]pyrimidin-3-yl)(4-(3-methoxyphenyl)piperazin-1-yl)methanone (39).: Yield: 85%. White solid. M.P. 60.1-61.8 °C. ^{1}H NMR (300 MHz, DMSO-*d*$_6$) δ (ppm): 8.38 (s, 1H), 7.07-7.13 (m, 3H), 7.01 (d, *J* = 7.8 Hz, 2H), 6.48-6.54 (m, 2H), 6.36-6.39 (m, 1H), 4.10 (s, 2H), 3.70 (m, 7H), 3.22

(s, 4H), 2.77 (s, 3H), 2.44 (s, 3H), 2.23 (s, 3H). ^{13}C NMR (75 MHz, DMSO-d_6) δ (ppm): 162.5, 160.6, 160.2, 152.2, 145.3, 144.5, 142.6, 135.3, 135.2, 129.6, 129.2, 127.7, 118.4, 108.3, 104.7, 104.5, 101.9, 54.8, 48.7 (br), 32.2, 23.7, 20.5, 13.6. IR ν_{max} (neat): 2920, 1615, 1594, 1549, 1481, 1445, 1382, 1256, 1191, 1163, 1024, 991, 840, 774. HRMS (ESI+): *m/z* [*M*+Na]$^+$ calcd. for $C_{28}H_{31}N_5O_2Na^+$, 492.2370; found, 492.2366 (error 0.80 ppm).

(5,7-dimethyl-6-(4-methylbenzyl)pyrazolo[1,5-a]pyrimidin-3-yl)(4-(m-tolyl)piperazin-1-yl)methano ne (40).: Yield: 79%. White solid. M.P. 78.9-80.5 °C. ^{1}H NMR (300 MHz, DMSO-d_6) δ (ppm): 8.37 (s, 1H), 7.07-7.11 (m, 3H), 7.02 (d, J = 7.8 Hz, 2H), 6.74-6.78 (m, 2H), 6.60-6.63 (m, 1H), 4.12 (s, 2H), 3.71 (s, 4H), 3.20 (s ,4H), 2.78 (s, 3H), 2.45 (s, 3H), 2.24-2.25 (m, 6H). ^{13}C NMR (75 MHz, DMSO-d_6) δ (ppm): 162.5, 160.6, 150.9, 145.3, 144.5, 142.7, 138.0, 135.3, 135.2, 129.2, 128.8, 127.7, 120.0, 118.4, 116.5, 113.0, 104.7, 48.8 (br), 32.2, 23.8, 21.4, 20.5, 13.7. IR ν_{max} (neat): 2920, 1669, 1615, 1600, 1547, 1433, 1385, 1241, 1193, 991, 836, 772, 693. HRMS (ESI+): *m/z* [*M*+Na]$^+$ calcd. for $C_{28}H_{31}N_5ONa^+$, 476.2421; found, 476.2408 (error 2.69 ppm).

(5,7-dimethyl-6-(4-methylbenzyl)pyrazolo[1,5-a]pyrimidin-3-yl)(4-(3-isopropylphenyl)piperazin-1-yl)methanone (41).: Yield: 75%. White solid. M.P. 78.9-80.5 °C. ^{1}H NMR (300 MHz, DMSO-d_6) δ (ppm): 8.38 (s, 1H), 7.08-7.15 (m, 3H), 7.02 (d, J = 7.7 Hz, 2H), 6.83 (s, 1H), 6.74-6.77 (m, 1H), 6.67-6.70 (m, 1H), 4.12 (s, 2H), 3.72 (s, 4H), 3.20 (s 4H), 2.78-2.84 (m, 4H), 2.45 (s, 3H), 2.24 (s, 3H), 1.16 (d, J = 6.8 Hz, 6H). ^{13}C NMR (75 MHz, DMSO-d_6) δ (ppm): 162.5, 160.6, 151.0, 149.2, 145.3, 144.5, 142.7, 135.3, 135.2, 129.2, 128.8, 127.7, 118.4, 117.3, 114.3, 113.4, 104.7, 49.0 (br), 33.7, 32.2, 23.9, 23.7, 20.5, 13.7. IR ν_{max} (neat): 2958, 1668, 1615, 1599, 1548, 1434, 1385, 1237, 1196, 993, 835, 776, 700. HRMS (ESI+): *m/z* [*M*+Na]$^+$ calcd. for $C_{30}H_{35}N_5ONa^+$, 504.2734; found, 504.2732 (error 0.36 ppm).

6-benzyl-5,7-dimethylpyrazolo[1,5-a]pyrimidine-3-carboxamide (42).: Yield: 60%. White solid. M.P. 245.5-248.0 °C. ^{1}H NMR (300 MHz, DMSO-d_6) δ (ppm): 8.46 (s, 1H), 7.57 (s, 1H), 7.42 (s, 1H), 7.26-7.31 (m, 2H), 7.18-7.23 (m, 1H), 7.12-7.15 (m, 2H), 4.20 (s, 2H), 2.79 (s, 3H), 2.50 (s, 3H). ^{13}C NMR (75 MHz, DMSO-d_6) δ (ppm): 163.0, 161.5, 145.5, 144.8, 144.0, 138.3, 128.7, 127.9, 126.4, 118.7, 104.4, 32.6, 23.7, 13.7. IR ν_{max} (neat): 3396, 3314, 3272, 3155, 2940, 1651, 1614, 1541, 1524, 1485, 1267, 1196, 797, 704, 635. HRMS (ESI+): *m/z* [2M+H]$^+$ calcd. for $C_{32}H_{33}N_8O_2^+$, 561.2721; found, 561.2708 (error 2.31 ppm).

6-benzyl-N-cyclohexyl-5,7-dimethylpyrazolo[1,5-a]pyrimidine-3-carboxamide (43).: Yield:57%. White solid. M.P. 180.1-181.8 °C. ^{1}H NMR (300 MHz, DMSO-d_6) δ (ppm): 8.46 (s, 1H), 8.07 (d, J = 7.7 Hz, 1H), 7.26-7.31 (m, 2H), 7.17-7.22 (m, 1H), 7.12-7.14 (m, 2H), 4.19 (s, 2H), 3.86 (m, 1H), 2.79 (s, 3H), 2.50 (s, 3H), 1.84-1.87 (m, 2H), 1.66 (m, 2H), 1.52 (m, 1H), 1.27-1.40 (m, 5H). ^{13}C NMR (75 MHz, DMSO-d_6) δ (ppm): 161.3, 160.4, 145.7, 144.4, 143.7, 138.2, 128.6, 127.8, 126.4, 118.7, 104.3, 46.4, 32.6, 32.4, 25.2, 24.0, 13.7. IR ν_{max} (neat): 3314, 2929, 2851, 1643, 1612, 1548, 1517, 1427, 1194, 778, 743, 703, 645. HRMS (ESI+): *m/z* [2M+H]$^+$ calcd. for $C_{44}H_{53}N_8O_2^+$, 725.4286; found, 725.4286 (error 0 ppm).

6-benzyl-5,7-dimethyl-N-phenylpyrazolo[1,5-a]pyrimidine-3-carboxamide (44).: Yield: 75%. White solid. M.P. 211.3-212.6 °C. ^{1}H NMR (300 MHz, DMSO-d_6) δ (ppm): 10.19 (s, 1H), 8.64 (s, 1H), 7.73-7.76 (m, 2H), 7.34-7.39 (m, 2H), 7.28-7.31 (m, 2H), 7.22-7.24 (m, 1H), 7.16-7.19 (m, 2H), 7.09 (m, 1H), 4.25 (s, 2H), 2.85 (s, 3H), 2.62 (s, 3H). ^{13}C NMR (75 MHz, DMSO-d_6) δ (ppm): 162.0, 159.8, 146.1, 144.9, 143.7, 138.8, 138.2, 129.0, 128.7, 127.9, 126.4, 123.3, 119.3, 119.1, 104.0, 32.6, 23.9, 13.8. IR ν_{max} (neat): 3297, 3256, 3197, 3146, 1779, 1662, 1600, 1543, 1499, 1481, 1381, 1312, 1257, 1196, 744, 706. HRMS (ESI+): *m/z* $[M+H]^+$ calcd. for $C_{22}H_{21}N_4O^+$, 357.1710; found, 357.1713 (error −0.88 ppm).

(6-benzyl-5,7-dimethylpyrazolo[1,5-a]pyrimidin-3-yl)(piperidin-1-yl)methanone (45).: Yield: 96%. White solid. M.P. 69.2-71.0 °C. ^{1}H NMR (500 MHz, DMSO-d_6) δ (ppm): 8.30 (s, 1H), 7.27-7.30 (m, 2H), 7.18-7.21 (m, 1H), 7.12-7.14 (m, 2H), 4.17 (s, 2H), 3.53 (brs, 4H), 2.77 (s, 3H), 2.44 (s, 3H), 1.59-1.61 (m, 2H), 1.55-1.56 (m, 4H). ^{13}C NMR (125 MHz, DMSO-d_6) δ (ppm): 162.3, 160.3, 144.9, 144.4, 142.6, 138.5, 128.6, 127.8, 126.3, 118.0, 105.3, 48.2 (br), 42.6 (br), 32.6, 25.8 (br), 24.1, 23.7, 13.7. IR ν_{max} (neat): 2933, 2853, 1733, 1674, 1614, 1547, 1434, 1386, 1252, 982, 835, 770, 734, 703, 655. HRMS (ESI+): *m/z* $[2M+Na]^+$ calcd. for $C_{42}H_{48}N_8O_2Na^+$, 719.3792; found, 719.3792 (error 0 ppm).

tert-Butyl 4-(6-benzyl-5,7-dimethylpyrazolo[1,5-a]pyrimidine-3-carbonyl)piperazine-1-carboxylate (46).: Yield: 86%. White solid. M.P. 186.3-188.8 °C. ^{1}H NMR (300 MHz, DMSO-d_6) δ (ppm): 8.35 (s, 1H); 7.27-7.31 (m, 2H), 7.21-7.23 (m, 1H), 7.13-7.15 (m, 2H), 4.18 (s, 2H), 3.55(s, 4H), 3.44(s, 4H), 2.78 (s, 3H), 2.46 (s, 3H), 1.41 (s, 9H). ^{13}C NMR (75 MHz, DMSO-d_6) δ (ppm): 162.7, 160.7, 153.8, 145.4, 144.7, 142.7, 138.4, 128.7, 127.9, 126.3, 118.3, 104.6, 79.1, 43.8, 32.6, 28.0, 23.8, 13.7. IR ν_{max} (neat): 3100, 2990, 2851, 1697, 1609, 1541, 1418, 1364, 1237, 1166, 837, 772, 742, 708, 657. HRMS (ESI): *m/z* $[M+H]^+$ calcd. for $C_{25}H_{32}N_5O_3^+$, 450.2500; found, 450.2508 (error −1.85 ppm).

(6-benzyl-5,7-dimethylpyrazolo[1,5-a]pyrimidin-3-yl)(piperazin-1-yl)methanone (47).: *tert*-Butyl 4-(6-benzyl-5,7-dimethylpyrazolo[1,5-*a*]pyrimidine-3-carbonyl)piperazine-1-carboxylate **46** (600 mg, 1.33 mmol, 1.0 eq.) was dissolved in 6 mL of 4 M HCl in EtOAc. The solution was stirred at room temperature for 4h, and then the solvent was removed *in vacuo*. The residue was partitioned between 30 mL DCM and 30 mL saturated sodium bicarbonate. The aqueous layer was extracted with DCM (20 mL×2). The combined organic layers were dried over anhydrous Na_2SO_4 and concentrated *in vacuo* to give compound **47** (173 mg, 0.49 mmol). Yield: 37%. White solid. M.P. 53.7-55.4 °C. ^{1}H NMR (300 MHz, DMSO-d_6) δ (ppm): 8.32 (s, 1H), 7.26-7.30 (m, 2H), 7.17-7.22 (m, 1H), 7.12-7.14 (m, 2H), 4.16 (s, 2H), 3.49 (s, 4H), 2.88-2.98 (m, 1H), 2.77 (s, 3H), 2.74 (s, 4H), 2.44 (s, 3H). ^{13}C NMR (75 MHz, DMSO-d_6) δ (ppm): 162.4, 160.3, 145.0, 144.5, 142.6, 138.4, 128.6, 127.8, 126.3, 118.0, 105.0, 45.9, 32.6, 23.7, 13.6. IR ν_{max} (neat): 3491, 3311, 2918, 2852, 1732, 1614, 1547, 1427, 1386, 1230, 1192, 1027, 988, 769, 735, 705. HRMS (ESI+): *m/z* $[M+H]^+$ calcd. for $C_{20}H_{24}N_5O^+$, 350.1975; found, 350.1981 (error −1.61 ppm).

(6-benzyl-5,7-dimethylpyrazolo[1,5-a]pyrimidin-3-yl)(4-(prop-2-yn-1-yl)piperazin-1-yl)methanone (48).: (6-benzyl-5,7-dimethylpyrazolo[1,5-a]pyrimidin-3-yl)(piperazin-1-

yl)methanone **47** (240 mg, 0.69 mmol, 1.0 eq.) was dissolved in anhydrous DCM (10 mL), and anhydrous K_2CO_3 (477 mg, 3.45 mmol, 5.0 eq.) was added. The mixture was vigorously stirred at room temperature, and neat propargyl bromide (204 mg, 1.72 mmol, 2.5 eq.) was added. The reaction was stirred at room temperature overnight, K_2CO_3 was filtered, and the filtrate was concentrated *in vacuo*. The residue was purified by column chromatography (silica gel, Dichloromethane/Methanol, 200:1 to 30:1) to give compound **48**. (36 mg, 0.09 mmol) Yield: 13%. White solid. M.P. 177.2-179.3 °C. ^{1}H NMR (500 MHz, DMSO-d_6) δ (ppm): 8.34 (s, 1H), 7.29 (m, 2H), 7.20 (m, 1H), 7.13-7.14 (m, 2H), 4.18 (s, 2H), 3.59 (brs, 4H), 3.32 (d, J = 2.2 Hz, 2H), 3.18 (t, J = 2.2 Hz, 1H), 2.77 (s, 3H), 2.52-2.54 (m, 4H), 2.45 (s, 3H). ^{13}C NMR (125 MHz, DMSO-d_6) δ (ppm): 162.5, 160.6, 145.2, 144.6, 142.7, 138.5, 128.7, 127.9, 126.4, 118.2, 104.8, 79.1, 76.0, 51.6, 47.1, 46.0, 41.8, 32.6, 23.8, 13.7. IR ν_{max} (neat): 3290, 3023, 2993, 2922, 2856, 2828, 1614, 1552, 1451, 1430, 1376, 1234, 1193, 1138, 1000, 888, 709. HRMS (ESI+): *m/z* $[2M+H]^+$ calcd. for $C_{46}H_{51}N_{10}O_2^+$, 775.4191; found, 775.4191 (error 0 ppm).

4.2 Docking-Based Virtual Screening

The NCI compound library containing approximately 260,000 compounds was screened through the MTiOpen screen automated virtual screening platform using the integrated Vina AutoDock program against RUVBL1/2 complex (PDB code: 5oaf) [38, 39]. The duplicate compounds were removed using Mona [40]. The 3D structure of all the compounds were generated and the energy minimization was performed by Frog2 [41]. The settings for compound library filters were as follows: the number of hydrogen bond acceptors < 10, the number of hydrogen bonds donors < 5, LogP < 5, molecular weight < 500, the number of rotatable bonds < 10, the topological polar surface area <140 [42]. The Grid center coordinates were 14.5666, 189.849, and 166.659. The sizes of the search space [Å] was 50 × 50 × 50. The top 3,000 results were visualized, and 80 compounds were selected to evaluate the inhibition activity against RUVBL1/2 complex.

4.3 Molecular cloning and Sequencing

The cDNA sequences of RUVBL1 and RUVBL2 were amplified using Platinum SuperFi PCR Master Mix (Thermofisher, Cat. No. 12358-010). PCR product was purified after electrophoresis through 0.8% Agarose and extracted using QIAquick Gel Extraction kit (QIAGEN, Cat. No. 28115). Both RUVBL1 and RUVBL2 were inserted into pCOLA-duet vector by Gibson assembly. Molecular cloning was performed using a NEB PCR Cloning Kit (Biolabs, NEB #E1202) according to the manufacturer's protocol. After overnight incubation, 5 clones were picked and plasmids were purified using a Plasmid miniprep kit (Bioland, Cat. No. PD01-01). Purified plasmids were sequenced by Sanger sequencing. PCR and sequencing primers are listed in Tables S4 and S5.

4.4 Expression and Purification of Recombinant Protein

Full-length recombinant His6x-tagged human RUVBL1 and RUVBL2 were expressed in E. coli Rosetta cells. The Rosetta cells were suspended in lysis buffer composed of 20 mM Tris, pH 8.0, 200 mM NaCl, 4 mM $MgCl_2$, 20 mM imidazole, β-mercaptoethanol, 50 mL/pill protease inhibitor, and 5% glycerol. The cell suspension was sonicated for three rounds

at 65, 70 and 70 amp, respectively. The mixture was then centrifuged for 1.5 hours at 15000 x g. The resulting supernatant was loaded onto a Ni-NTA column and eluted with a linear gradient of imidazole (0 min, 20 mM Tris pH 8.0, 300 mM NaCl, 4 mM $MgCl_2$, 20 mM Imidazole, 1 mM DTT, and 5% glycerol; 50 min, 20 mM Tris pH 8.0, 300 mM NaCl, 4 mM $MgCl_2$, 400 mM Imidazole, 1 mM DTT, and 5% glycerol; 60 min, 20 mM Tris pH 8.0, 300 mM NaCl, 4 mM $MgCl_2$, 400 mM Imidazole, 1 mM DTT, and 5% glycerol). SDS-Page was employed to probe the fractions containing RUVBL1/2 complex. The RUVBL1/2 solution was condensed and further purified by size-exclusion chromatography in 20 mM Tris pH 7.5, 300 mM sodium chloride, 1 mM magnesium chloride, 1 mM DTT, and 10% glycerol using a Superose 6 Increase 10/300 GL column (GE Healthcare), and stored in aliquots at −80 °C with glycerol.

4.5 ATPase Assay

The purified protein was assayed in 50 μL ATPase assay buffer (50 mM Tris pH 7.4, 20 mM $MgCl_2$, 0.1% Glycerol, and 0.01% Triton X-100) containing 200 μM ATP. After 70 min incubation at 37 °C, 50 μL Biomol Green reagent (Enzo Life Sciences) was added to quench the reaction, and the absorbance at 635 nm was measured using a BioTek Synergy Neo 2 plate reader. The eight-dose titrations (0, 2.00, 6.58, 9.88, 14.81, 22.22, 33.33, 50.00 μM) were performed of the compound to the reaction to determine the IC_{50} values of the compounds. In this assay, the concentration of RUVBL1/2, RUVBL, and RUVBL2 were 0.05 μM, 1.0 μM, and 3.0 μM, respectively. The results were calculated from six replicates using GraphPad Prism 7.0.

4.6 Antiproliferative assay

Cell viability was measured using CellTiter Glo® Luminescent Cell Viability Assay (Promega) according to the manufacturer's procedure. RMPI1640 or DMEM containing 5% FBS and 1% Penicillin Streptomycin (Thermo Fisher) was used as cell viability assay medium. To find the linear relationship between the relative luminescence unit and the number of viable cells, a standard curve for each cell line was generated. Generally, 30 μL of cell suspension was plated in 384-well white plates (Greiner) with serial 2-fold dilution (from 30000 to 284 cells per well). Twenty-four hours after seeding, 8 μL of assay media containing 5% DMSO was added into each well and plates were incubated for an additional 48 h at 37 °C in a 5% CO_2 incubator. To test the anti-proliferative activity of RUVBL1/2 complex inhibitors, cells were seeded at 750 to 3000 cells per well according to the linear range determined from the standard curve of each cell line. Twenty-four hours after seeding, cells were treated with the compounds (three-fold dilution, eight concentrations). After 48 hours of treatment, cell viability was measured using CellTiter Glo and IC_{50} values were calculated using the percentage of growth of treated cells versus the DMSO control.

4.7 Proteomics

HCT116 cells were treated with DMSO, 15 μM or 30 μM tested compound for 24 h, and pellets were harvested. The LC-MS samples were prepared by following the instructions of Thermo EasyPep Mini MS Sample Prep Kit (REF A4006) and peptide concentration was tested through Pierce Quantitative Fluorometric Peptide Assay (cat# 23290).

The LC-MS/MS experiments were performed using an EASY-nLC 1000 (ThermoFisher Scientific, San Jose, CA) connected to an Orbitrap Eclipse Tribrid mass spectrometer (Thermo Fisher Scientific, San Jose, CA). The sample (1 μg) in 0.1% FA solution was loaded onto an Aurora UHPLC Column (25 cm x 75 μm, 1.6 μm C18, AUR2-25075C18A, Ion Opticks) and separated over 136 min at a flow rate of 0.35 μL/min with the following gradient: 2-6% Solvent B (7.5 min), 6-25% B (82.5 min), 25-40% B (30 min), 40-98% B (1 min), and 98% B (15 min). Solvent A consisted of 97.9% H_2O, 2% ACN, and 0.1% formic acid, and solvent B consisted of 19.9% H_2O, 80% ACN, and 0.1% formic acid. An MS1 scan was acquired in the Orbitrap at 120,000 resolution with a scan range of 350-1500 m/z. The AGC target was $4x10^5$, and the maximum injection time was 50 mins. Dynamic exclusion was set to exclude features after 1 time for 60 s with a 10-ppm mass tolerance. Higher-energy collisional dissociation (HCD) fragmentation was performed with 35% collision energy after quadruple isolation of features using a 1.6 m/z isolation window, $5×10^4$ AGC target, and 35 ms maximum injection time. MS2 scans were then also acquired by the Orbitrap with 50,000 resolution. Ion source settings were as follows: ion source type, NSI; spray voltage, 2400 V; ion transfer tube temperature, 275 °C. System control and data collection were performed using Xcalibur software.

The proteomic analysis was performed through Proteome Discoverer 2.4 (Thermo Scientific) using the Uniprot human database and the Byonic search algorithm (Protein Metrics). Percolator FDRs were set at 0.001 (strict) and 0.01 (relaxed). Peptide FDRs were set at 0.001 (strict) and 0.01 (relaxed), with medium confidence and a minimum peptide length of 6. Normalization was performed on the total peptide amount. The limma analysis was performed using R studio following the user guide [43]. The volcano and heatmap figures were plotted by GraphPad Prism 7.0. The Venn diagram was plotted using an online tool (http://bioinformatics.psb.ugent.be/webtools/Venn/).

4.8 GO and KEGG pathway analysis of the differentially expressed proteins

The DAVID 6.8 database (https://david.ncifcrf.gov/) was employed to perform GO functional and KEGG pathway analysis of the integrated differentially expressed proteins [44]. The GO functional analysis of the integrated differentially expressed proteins involves three parts: biological process, cellular component and molecular function. The bubble graph was plotted by http://www.bioinformatics.com.cn, an online platform for data analysis and visualization.

Supplementary Material

Refer to Web version on PubMed Central for supplementary material.

Acknowledgments

This work was supported in part by the National Institute of Child Health and Human Development R01 HD086596 and The Cultivation Fund of School of Pharmaceutical Sciences, Capital Medical University (2021).

References

[1]. Jha S, Dutta A, RVB1/RVB2: running rings around molecular biology, Mol. Cell, 34 (2009) 521–533. [PubMed: 19524533]

[2]. Venteicher AS, Meng Z, Mason PJ, Veenstra TD, Artandi SE, Identification of ATPases pontin and reptin as telomerase components essential for holoenzyme assembly, Cell, 132 (2008) 945–957. [PubMed: 18358808]

[3]. Grigoletto A, Lestienne P, Rosenbaum J, The multifaceted proteins Reptin and Pontin as major players in cancer, Biochim. Biophys. Acta, 1815 (2011) 147–157. [PubMed: 21111787]

[4]. Jha S, Gupta A, Dar A, Dutta A, RVBs are required for assembling a functional TIP60 complex, Mol. Cell Biol, 33 (2013) 1164–1174. [PubMed: 23297341]

[5]. Tosi A, Haas C, Herzog F, Gilmozzi A, Berninghausen O, Ungewickell C, Gerhold CB, Lakomek K, Aebersold R, Beckmann R, Hopfner KP, Structure and subunit topology of the INO80 chromatin remodeler and its nucleosome complex, Cell, 154 (2013) 1207–1219. [PubMed: 24034245]

[6]. Nguyen VQ, Ranjan A, Stengel F, Wei D, Aebersold R, Wu C, Leschziner AE, Molecular architecture of the ATP-dependent chromatin-remodeling complex SWR1, Cell, 154 (2013) 1220–1231. [PubMed: 24034246]

[7]. Kakihara Y, Houry WA, The R2TP complex: discovery and functions, Biochim. Biophys. Acta, 1823 (2012) 101–107. [PubMed: 21925213]

[8]. Yenerall P, Das AK, Wang S, Kollipara RK, Li LS, Villalobos P, Flaming J, Lin YF, Huffman K, Timmons BC, Gilbreath C, Sonavane R, Kinch LN, Rodriguez-Canales J, Moran C, Behrens C, Hirasawa M, Takata T, Murakami R, Iwanaga K, Chen BPC, Grishin NV, Raj GV, Wistuba II, Minna JD, Kittler R, RUVBL1/RUVBL2 ATPase Activity Drives PAQosome Maturation, DNA Replication and Radioresistance in Lung Cancer, Cell Chem. Biol, 27 (2020) 105–121. e14. [PubMed: 31883965]

[9]. Nano N, Houry WA, Chaperone-like activity of the AAA+ proteins Rvb1 and Rvb2 in the assembly of various complexes, Philos. Trans. R. Soc. Lond., B, Biol. Sci, 368 (2013) 20110399. [PubMed: 23530256]

[10]. Machado-Pinilla R, Liger D, Leulliot N, Meier UT, Mechanism of the AAA+ ATPases pontin and reptin in the biogenesis of H/ACA RNPs, RNA, 18 (2012) 1833–1845. [PubMed: 22923768]

[11]. Rottbauer W, Saurin AJ, Lickert H, Shen X, Burns CG, Wo ZG, Kemler R, Kingston R, Wu C, Fishman M, Reptin and Pontin Antagonistically Regulate Heart Growth in Zebrafish Embryos, Cell, 111 (2002) 661–672. [PubMed: 12464178]

[12]. Lee JS, Kim Y, Kim IS, Kim B, Choi HJ, Lee JM, Shin HJ, Kim JH, Kim JY, Seo SB, Lee H, Binda O, Gozani O, Semenza GL, Kim M, Kim KI, Hwang D, Baek SH, Negative regulation of hypoxic responses via induced Reptin methylation, Mol. Cell, 39 (2010) 71–85. [PubMed: 20603076]

[13]. Lee JS, Kim Y, Bhin J, Shin HJ, Nam HJ, Lee SH, Yoon JB, Binda O, Gozani O, Hwang D, Baek SH, Hypoxia-induced methylation of a pontin chromatin remodeling factor, Proc. Natl. Acad. Sci. U. S. A, 108 (2011) 13510–13515. [PubMed: 21825155]

[14]. Torreira E, Jha S, Lopez-Blanco JR, Arias-Palomo E, Chacon P, Canas C, Ayora S, Dutta A, Llorca O, Architecture of the pontin/reptin complex, essential in the assembly of several macromolecular complexes, Structure, 16 (2008) 1511–1520. [PubMed: 18940606]

[15]. Gorynia S, Bandeiras TM, Pinho FG, McVey CE, Vonrhein C, Round A, Svergun DI, Donner P, Matias PM, Carrondo MA, Structural and functional insights into a dodecameric molecular machine - the RuvBL1/RuvBL2 complex, J. Struct. Biol, 176 (2011) 279–291. [PubMed: 21933716]

[16]. Petukhov M, Dagkessamanskaja A, Bommer M, Barrett T, Tsaneva I, Yakimov A, Queval R, Shvetsov A, Khodorkovskiy M, Kas E, Grigoriev M, Large-scale conformational flexibility determines the properties of AAA+ TIP49 ATPases, Structure, 20 (2012) 1321–1331. [PubMed: 22748767]

[17]. Cheung KL, Huen J, Houry WA, Ortega J, Comparison of the multiple oligomeric structures observed for the Rvb1 and Rvb2 proteins, Biochem. Cell Biol, 88 (2010) 77–88. [PubMed: 20130681]

[18]. Lauscher JC, Loddenkemper C, Kosel L, Grone J, Buhr HJ, Huber O, Increased pontin expression in human colorectal cancer tissue, Hum. Pathol, 38 (2007) 978–985. [PubMed: 17442372]

[19]. Huber O, Menard L, Haurie V, Nicou A, Taras D, Rosenbaum J, Pontin and reptin, two related ATPases with multiple roles in cancer, Cancer Res., 68 (2008) 6873–6876. [PubMed: 18757398]

[20]. Lauscher JC, Elezkurtaj S, Dullat S, Lipka S, Grone J, Buhr HJ, Huber O, Kruschewski M, Increased Pontin expression is a potential predictor for outcome in sporadic colorectal carcinoma, Oncol. Rep, 28 (2012) 1619–1624. [PubMed: 22895545]

[21]. Haurie V, Menard L, Nicou A, Touriol C, Metzler P, Fernandez J, Taras D, Lestienne P, Balabaud C, Bioulac-Sage P, Prats H, Zucman-Rossi J, Rosenbaum J, Adenosine triphosphatase pontin is overexpressed in hepatocellular carcinoma and coregulated with reptin through a new posttranslational mechanism, Hepatology, 50 (2009) 1871–1883. [PubMed: 19877184]

[22]. Grigoletto A, Neaud V, Allain-Courtois N, Lestienne P, Rosenbaum J, The ATPase activity of reptin is required for its effects on tumor cell growth and viability in hepatocellular carcinoma, Mol. Cancer Res, 11 (2013) 133–139. [PubMed: 23233483]

[23]. Menard L, Taras D, Grigoletto A, Haurie V, Nicou A, Dugot-Senant N, Costet P, Rousseau B, Rosenbaum J, In vivo silencing of Reptin blocks the progression of human hepatocellular carcinoma in xenografts and is associated with replicative senescence, J. Hepatol, 52 (2010) 681–689. [PubMed: 20346530]

[24]. Breig O, Bras S, Martinez Soria N, Osman D, Heidenreich O, Haenlin M, Waltzer L, Pontin is a critical regulator for AML1-ETO-induced leukemia, Leukemia, 28 (2014) 1271–1279. [PubMed: 24342949]

[25]. Elkaim J, Castroviejo M, Bennani D, Taouji S, Allain N, Laguerre M, Rosenbaum J, Dessolin J, Lestienne P, First identification of small-molecule inhibitors of Pontin by combining virtual screening and enzymatic assay, Biochem. J, 443 (2012) 549–559. [PubMed: 22273052]

[26]. Elkaim J, Lamblin M, Laguerre M, Rosenbaum J, Lestienne P, Eloy L, Cresteil T, Felpin FX, Dessolin J, Design, synthesis and biological evaluation of Pontin ATPase inhibitors through a molecular docking approach, Bioorg. Med. Chem. Lett, 24 (2014) 2512–2516. [PubMed: 24767849]

[27]. Ebisawa M, Suzuki T, Haginoya N, Hamada T, Murata T, Uoto K, Murakami R, Takata T, Aminopyrazolone derivative, CA2939687A1, 2017.

[28]. Izumi N, Yamashita A, Iwamatsu A, Kurata R, Nakamura H, Saari B, Hirano H, Anderson P, Ohno S, AAA+ proteins RUVBL1 and RUVBL2 coordinate PIKK activity and function in nonsense-mediated mRNA decay, Sci. Signal, 3 (2010) ra27. [PubMed: 20371770]

[29]. Nano N, Ugwu F, Seraphim TV, Li T, Azer G, Isaac M, Prakesch M, Barbosa LRS, Ramos CHI, Datti A, Houry WA, Sorafenib as an Inhibitor of RUVBL2, Biomolecules, 10 (2020) 605.

[30]. Wilhelm SM, Adnane L, Newell P, Villanueva A, Llovet JM, Lynch M, Preclinical overview of sorafenib, a multikinase inhibitor that targets both Raf and VEGF and PDGF receptor tyrosine kinase signaling, Mol. Cancer Ther, 7 (2008) 3129–3140. [PubMed: 18852116]

[31]. Assimon VA, Tang Y, Vargas JD, Lee GJ, Wu ZY, Lou K, Yao B, Menon MK, Pios A, Perez KC, Madriaga A, Buchowiecki PK, Rolfe M, Shawver L, Jiao X, Le Moigne R, Zhou HJ, Anderson DJ, CB-6644 Is a Selective Inhibitor of the RUVBL1/2 Complex with Anticancer Activity, ACS Chem. Biol, 14 (2019) 236–244. [PubMed: 30640450]

[32]. Morris GM, Huey R, Lindstrom W, Sanner MF, Belew RK, Goodsell DS, Olson AJ, AutoDock4 and AutoDockTools4: Automated docking with selective receptor flexibility, J. Comput. Chem, 30 (2009) 2785–2791. [PubMed: 19399780]

[33]. Zoete V, Daina A, Bovigny C, Michielin O, SwissSimilarity: A Web Tool for Low to Ultra High Throughput Ligand-Based Virtual Screening, J. Chem. Inf. Model, 56 (2016) 1399–1404. [PubMed: 27391578]

[34]. Wang R, Li X, Sun C, Yu L, Hua D, Shi C, Wang Q, Rao C, Luo W, Jiang Z, Zhou X, Yu S, The ATPase Pontin is a key cell cycle regulator by amplifying E2F1 transcription response in glioma, Cell Death Dis., 12 (2021) 141. [PubMed: 33542204]

[35]. Shen X, Mizuguchi G, Hamiche A, Wu C, A chromatin remodelling complex involved in transcription and DNA processing, Nature, 406 (2000) 541–544. [PubMed: 10952318]

[36]. Yenerall P, Das AK, Wang S, Kollipara RK, Li LS, Villalobos P, Flaming J, Lin YF, Huffman K, Timmons BC, Gilbreath C, Sonavane R, Kinch LN, Rodriguez-Canales J, Moran C, Behrens C, Hirasawa M, Takata T, Murakami R, Iwanaga K, Chen BPC, Grishin NV, Raj GV, Wistuba II, Minna JD, Kittler R, RUVBL1/RUVBL2 ATPase Activity Drives PAQosome Maturation, DNA Replication and Radioresistance in Lung Cancer, Cell Chem. Biol, 27 (2020) 105–121.e14. [PubMed: 31883965]

[37]. Zhang G, Li S, Cheng KW, Chou TF, AAA ATPases as therapeutic targets: Structure, functions, and small-molecule inhibitors, Eur. J. Med. Chem, 219 (2021) 113446. [PubMed: 33873056]

[38]. Labbe CM, Rey J, Lagorce D, Vavrusa M, Becot J, Sperandio O, Villoutreix BO, Tuffery P, Miteva MA, MTiOpenScreen: a web server for structure-based virtual screening, Nucleic Acids Res., 43 (2015) W448–454. [PubMed: 25855812]

[39]. Aramayo RJ, Willhoft O, Ayala R, Bythell-Douglas R, Wigley DB, Zhang X, Cryo-EM structures of the human INO80 chromatin-remodeling complex, Nat. Struct. Mol. Biol, 25 (2018) 37–44. [PubMed: 29323271]

[40]. Hilbig M, Rarey M, MONA 2: A Light Cheminformatics Platform for Interactive Compound Library Processing, J. Chem. Inf. Model., 55 (2015) 2071–2078. [PubMed: 26389652]

[41]. Miteva MA, Guyon F, Tuffery P, Frog2: Efficient 3D conformation ensemble generator for small compounds, Nucleic Acids Res., 38 (2010) W622–627. [PubMed: 20444874]

[42]. Veber DF, Johnson SR, Cheng HY, Smith BR, Ward KW, Kopple KD, Molecular properties that influence the oral bioavailability of drug candidates, J. Med. Chem, 45 (2002) 2615–2623. [PubMed: 12036371]

[43]. Smyth GK, Thorne NP, Wettenhall J, Limma: Linear Models for Microarray Data User's Guide. Software manual available from http://www.bioconductor.org., 2003.

[44]. Huang DW, Sherman BT, Zheng X, Yang J, Imamichi T, Stephens R, Lempicki RA, Extracting biological meaning from large gene lists with DAVID, Curr. Protoc. Bioinformatics, 27 (2009) 1–13.

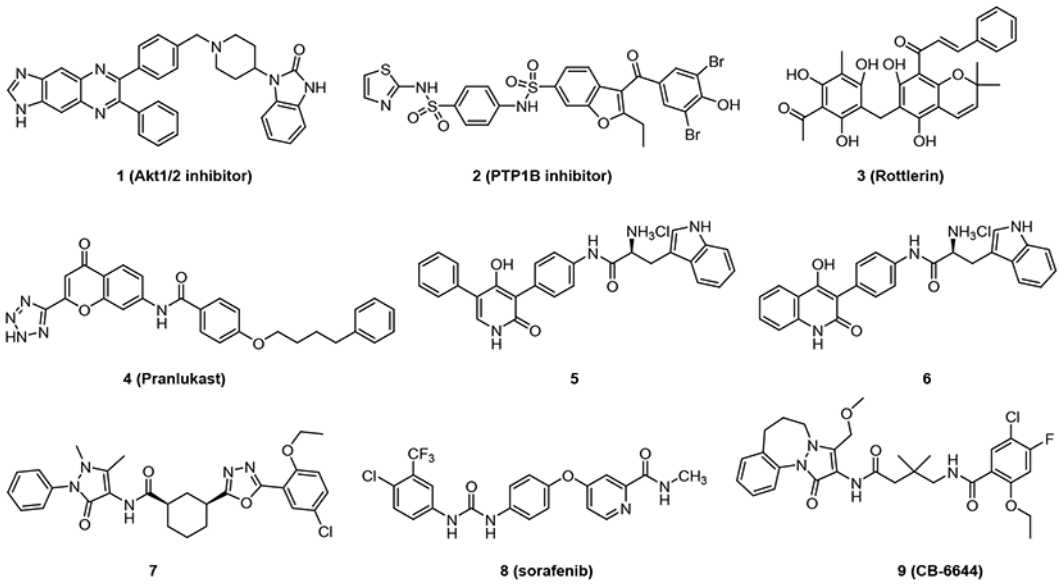

Figure 1.
Chemical Structures of known inhibitors against RUVBL proteins

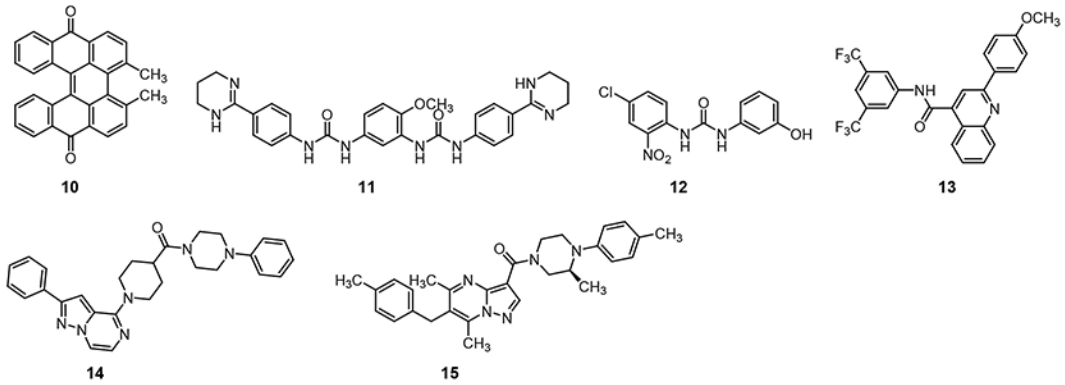

Figure 2.
Chemical Structure of compounds active against RUVBL1/2 complex

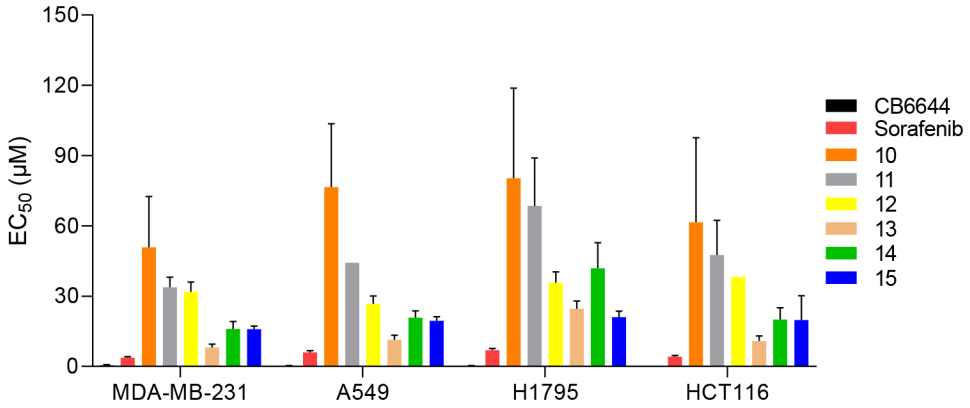

Figure 3.

Anti-proliferative effects of active molecules from virtual screening. Compounds **CB6644, 8 (Sorafenib), 10, 11, 12, 13, 14**, and **15** were evaluated for their anti-proliferative effects on breast cancer cell line MDA-MB-231, non-small cell lung cancer cell lines A549 and H1795, as well as human colon cancer cell line HCT116

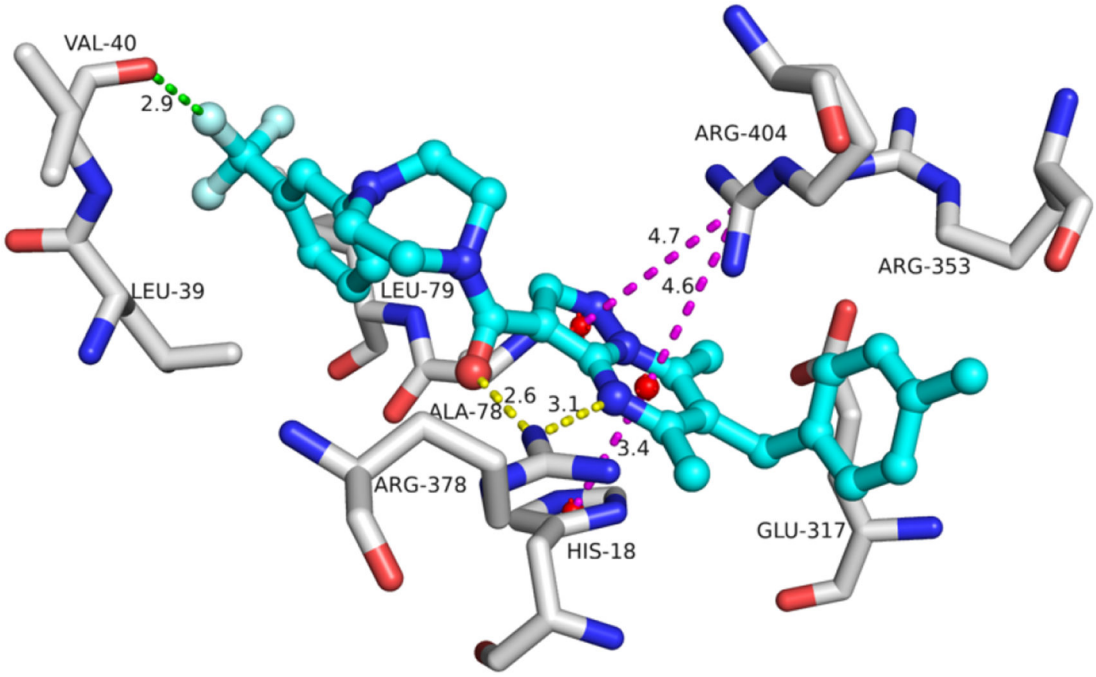

Figure 4.

Docking study of compound **18** with RUVBL1/2 (PDB code 5OAF). Compound **18** is presented as a cyan ball and stick model. Active residues are presented as gray sticks. Hydrogen bond, cation-π interaction, and halogen bond are presented as dashed yellow, magenta, and green lines, respectively.

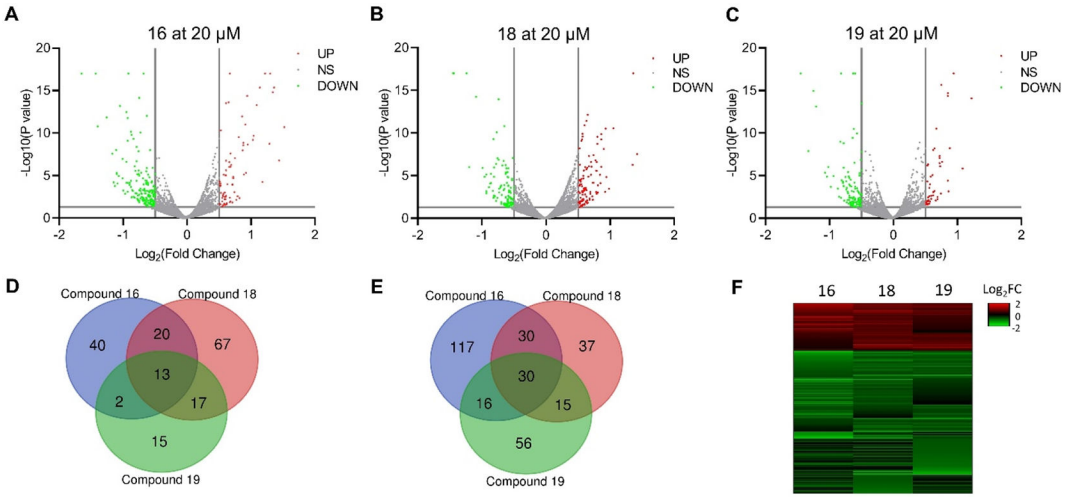

Figure 5.

Proteomic Effects of Compound Treatment. **A-C**) Volcano plots of the significantly differentially expressed proteins in HCT116 cells treated with **16, 18** and **19**, respectively. **D-E**) Venn diagrams of upregulated (D) and down-regulated (E) proteins ($p < 0.05$, $|Log_2FC|>0.5$) following treatment with **16, 18** and **19**, respectively. **F**) Heatmap of differentially regulated proteins from at least two compound-treated groups ($p < 0.05$, $|Log_2FC|>0.5$).

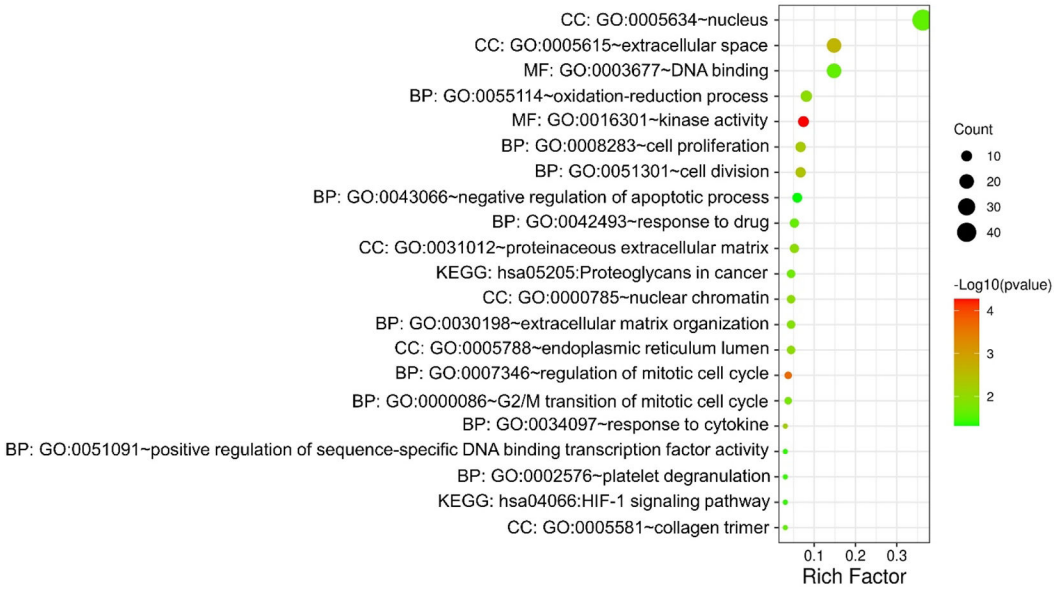

Figure 6.

GO and KEGG pathway enrichment analysis of the proteins dysregulated in at least two compound-treated samples. BP: biological progress; CC: cellular component; MF: molecular function.

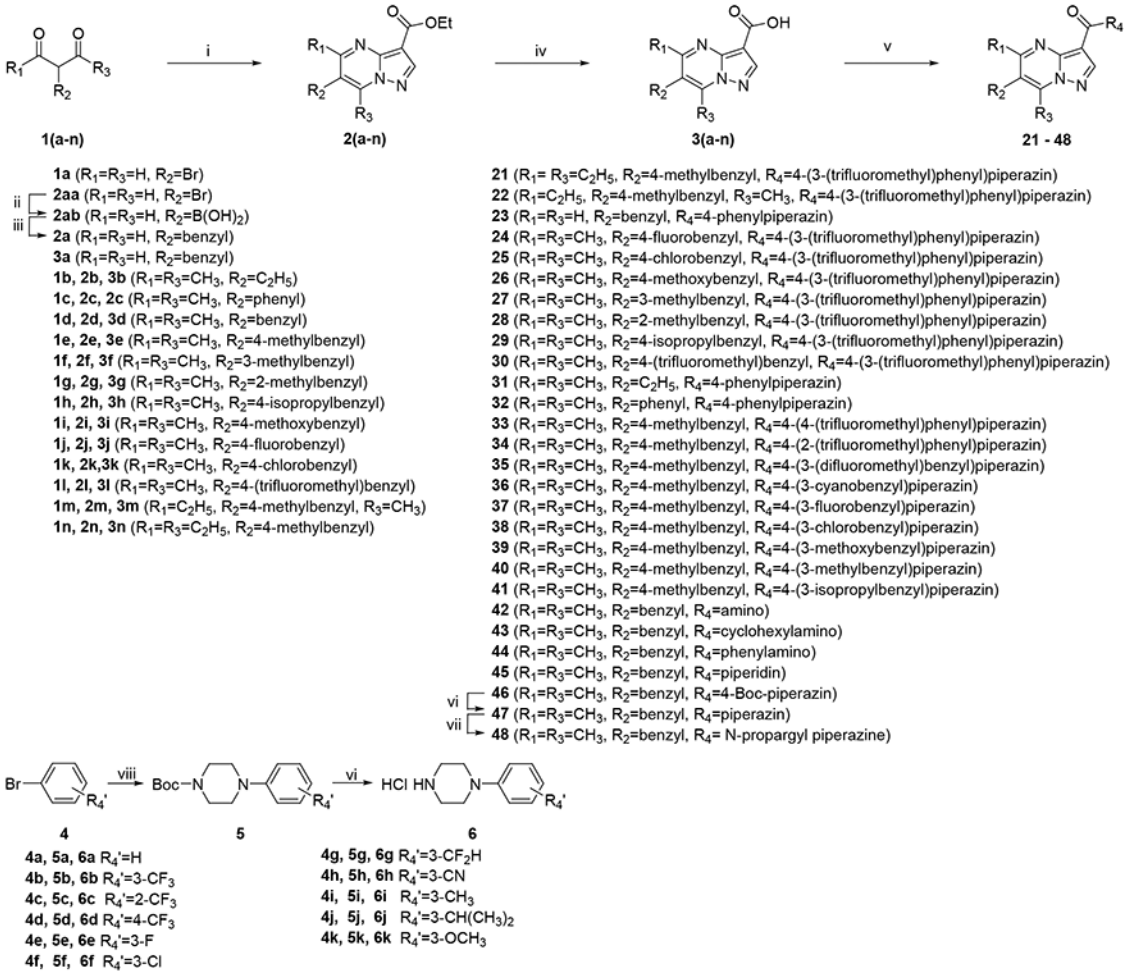

Scheme 1.

Representative Synthetic Route of pyrazolo[1,5-*a*]pyrimidine-3-carboxamides. Reagents and conditions: (i) ethyl 3-amino-1*H*-pyrazole-4-carboxylate, EtOH, AcOH, 70 °C , 3h; (ii) Bis(pinacolato)diboron, KOAc, $PdCl_2$(dppf)(DCM), Dioxane, 80 °C, overnight; (iii) Benzyl bromide, K_2CO_3, $PdCl_2$(dppf)(DCM), Dioxane, H_2O, 50 °C, overnight; (iv) 2 M NaOH, MeOH, THF, 56 °C, 3 h; (v) substituted amines **6a-k**, HATU, DIEA, DMF, rt, overnight; (vi) 4M HCl / EtOAc; (vii) propargyl bromide, K_2CO_3, DCM; (viii) *N*-Boc piperazine, $Pd(OAc)_2$, XPhos, KO*t*Bu, Dioxane, 90°C, 10h.

Table 1

The inhibitory activity of active compounds from virtual screening

Compounds	IC_{50} (μM)		
	RUVBL1/2	**RUVBL1**	**RUVBL2**
CB-6644	6.1 ± 0.5	> 66	> 66
8	55 ± 9.0	> 66	> 66
10	77 ± 24	> 66	> 66
11	46 ± 1.1	39 ± 7.7	> 66
12	68 ± 11	> 66	> 66
13	47± 2.0	26 ± 7.2	> 66
14	35 ± 6.4	31 ± 10	> 66
15	36 ± 2.1	65 ± 11	29 ± 7.4

Table 2

The anti-proliferative effects of pyrazolo[1,5-*a*]pyrimidine-3-carboxamides

Cmpds	IC_{50} (μM)			
	A549	HCT116	H1795	MDA-MB-231
CB-6644	0.3 ± 0.07	0.08 ± 0.01	0.26 ± 0.07	0.70 ± 0.29
16	26 ± 5.5	21 ± 4.5	25 ± 12	22 ± 4.3
17	32 ± 1.6	32 ± 3.8	46 ± 5.5	37 ± 8.2
18	15 ± 1.2	11 ± 1.0	15 ± 1.8	8.9 ± 0.9
19	17 ± 1.7	17 ± 5.4	19 ± 4.1	18 ± 3.8